Technical Appendix:
Demographic Aging and Long-Run Economic Growth in Germany

Christian Ochsner*)
Lars Other*)
Esther Thiel*)
Christopher Zuber*)

Appendix to the Working Paper 02/2024**)
February 2024

*) German Council of Economic Experts, E-Mail: christian.ochsner@svr-wirtschaft.de; lars.other@svr-wirtschaft.de; esther.thiel@svr-wirtschaft.de; christopher.zuber@svr-wirtschaft.de

**) The Appendix to the Working paper 02/2024 reflects the personal views of the authors and not necessarily those of the German Council of Economic Experts.

Technical Appendix

Demographic Aging and Long-Run Economic Growth in Germany*

Christian Ochsner† Lars Other‡

Esther Thiel§ Christopher Zuber¶

German Council of Economic Experts

February 19, 2024

*We thank Niklas Garnadt, Michael Kogler, Thilo Kroeger, Christian Matthes, Leonard Salzmann as well as Jens Boysen-Hogrefe, Kai Carstensen, Stefan Kooths, Timo Hoffman and other workshop participants the Kiel Institute for the World Economy as well as Rolf Strauch, Konstantinos Theodoridis and other workshop participants at the European Stability Mechanism and participants at the 17th International Conference for Computational and Financial Econometrics for numerous very helpful comments. In addition, we thank Waldemar Hamm, Antonia Koch and Lotte Nacke for research assistance and Michael Schidlowski and the Federal Statistical Office as well as Susanne Wanger and the Institute for Employment Research for immensely valuable help with the data. Finally, we are grateful the council members Veronika Grimm, Ulrike Malmendier, Achim Truger, Monika Schnitzer and Martin Werding for useful discussion. The views expressed here are those of the authors and not necessarily those of the GCEE.

†Email: christian.ochsner@svr-wirtschaft.de; corresponding author.

‡Email: lars.other@svr-wirtschaft.de

§Email: esther.thiel@svr-wirtschaft.de.

¶Email: christopher.zuber@svr-wirtschaft.de.

Contents

I Brief Model Summary

To improve overall accessibility, this appendix briefly reproduces the entire model. We aim to decompose observed output (approximated by gross domestic product), denoted as $\boldsymbol{y}$, into two distinct components: potential output $\bar{\boldsymbol{y}}$ and the output gap $\tilde{\boldsymbol{y}}$. The model structure is adopted from Havik, McMorrow, Orlandi, Planas, Raciborski, Roeger, Rossi, Thum-Thysena, and Vandermeulen (2014) as well as Breuer and Elstner (2020) and augmented with human capital. To identify potential output, we estimate the model given by

$$\bar{\boldsymbol{y}} = \bar{\boldsymbol{a}}(\bar{\boldsymbol{h}}\bar{\boldsymbol{l}})^{\boldsymbol{\alpha}}\bar{\boldsymbol{k}}^{(\boldsymbol{1}_T-\boldsymbol{\alpha})} \tag{1}$$

$$\bar{\boldsymbol{l}} = \boldsymbol{b}\bar{\boldsymbol{w}}(\boldsymbol{1}_T - \bar{\boldsymbol{u}})\bar{\boldsymbol{s}} \tag{2}$$

$$\bar{\boldsymbol{w}} = \sum_{i=1}^{5} \bar{\boldsymbol{b}}_i \bar{\boldsymbol{b}}^{-1} \bar{\boldsymbol{w}}_i \tag{3}$$

$$\bar{\boldsymbol{s}} = \bar{\boldsymbol{s}}^s \bar{\boldsymbol{q}}^s + (\boldsymbol{1}_T - \bar{\boldsymbol{q}}^s)(\bar{\boldsymbol{s}}^p \bar{\boldsymbol{q}}^p + (\boldsymbol{1}_T - \bar{\boldsymbol{q}}^p)\bar{\boldsymbol{s}}^f) \tag{4}$$

$$\bar{\boldsymbol{h}} = \exp\{\beta \boldsymbol{x}\} \tag{5}$$

$$\dot{\bar{\boldsymbol{k}}} = \sum_{j=1}^{4} \dot{\boldsymbol{v}}^j (\frac{\boldsymbol{c}^j}{\boldsymbol{c}^{j-}})^{-1} \tag{6}$$

$$\dot{\boldsymbol{v}}^j = \dot{\boldsymbol{v}}^{j+} - \dot{\boldsymbol{v}}^{j-} \tag{7}$$

$$\dot{\boldsymbol{z}}^j = \dot{\boldsymbol{v}}^{j+} - \dot{\boldsymbol{z}}^{j-} \tag{8}$$

$$\bar{\boldsymbol{c}}^j = \max(\boldsymbol{0}_T, \bar{\boldsymbol{r}} + \bar{\boldsymbol{\delta}}^j - \mathbb{E}(\bar{\boldsymbol{d}}^j)) \tag{9}$$

$$\boldsymbol{r} = (\boldsymbol{1}_T - \boldsymbol{\alpha})\boldsymbol{y}\boldsymbol{v}^{-1} + \boldsymbol{d} \tag{10}$$

where, in Eq. (1), $\bar{\boldsymbol{y}}$, $\bar{\boldsymbol{a}}$, $\bar{\boldsymbol{h}}$, $\bar{\boldsymbol{l}}$ and $\bar{\boldsymbol{k}}$ are a $T \times 1$ vectors of potential output, potential total factor productivity, potential human capital, potential labor and potential capital use. $0 \leq \alpha \leq 1$ is a known constant, namely the output elasticity of labor. We set $\alpha = 0.66$, which is broadly in line with the sample period average of the labor share of gross value added in Germany. $\boldsymbol{1}_T$ is the $T \times 1$ unit vector.

In Eqs. (2)–(5), which specify the labor component of the model,

- $\bar{\boldsymbol{l}}$ is the potential labor volume
- $\bar{\boldsymbol{b}}$ is the potential working age population
- $\bar{\boldsymbol{w}}$ is potential aggregate labor participation
- $\bar{\boldsymbol{w}}_i$ and $\bar{\boldsymbol{b}}_i$ denote potential labor participation of age group i as well as the share of age group i of the working age population
- $\bar{\boldsymbol{s}}$ is the potential of total number of hours worked
- $\bar{\boldsymbol{s}}^p$ is the potential of number of hours worked by part-time employees
- $\bar{\boldsymbol{s}}^s$ is the potential of number of hours worked by self-employed persons
- $\bar{\boldsymbol{s}}^f$ is the potential of number of hours worked by full-time employees
- $\bar{\boldsymbol{q}}^s$ is the rate of self-employment
- $\bar{\boldsymbol{q}}^p$ is the rate of part-time employment
- $\bar{\boldsymbol{u}}$ is the non-accelerating rate of unemployment
- β is the marginal percentage rate of return to education in Germany (we set $\beta = 9$, which is broadly in line with Anger, Plünnecke, and Schmidt (2010) and Pfeiffer and Stichnoth (2021))
- $\boldsymbol{x}$ is the average number of years of schooling, which is derived from the data of de la Fuente and Doménech (2006) and interpolated to yearly frequency by means of polynomial smoothing.

In Eqs. (6)–(10), which summarize the capital component of the model,

- $\dot{}$ denotes growth rates
- $\boldsymbol{k}^j$ denotes use of capital
- $\boldsymbol{v}^j$ denotes real gross fixed assets of capital good j (equipment, other capital, residential and nonresidential capital)
- $\boldsymbol{v}^{+j}$ denotes real additions to gross fixed assets of capital good j
- $\boldsymbol{v}^{-j}$ denotes real disposals from gross fixed assets of capital good j
- $\boldsymbol{z}^j$ denotes real net fixed assets of capital good j
- $\boldsymbol{v}^{-j}$ denotes real depreciation of net fixed assets of capital good j
- $\boldsymbol{c}^j$ denotes capital costs of capital good j
- $\boldsymbol{c}^{j-}$ denotes total capital costs less than capital costs of capital good j
- $\boldsymbol{r}$ is the required return to capital
- $\boldsymbol{\delta}^j$ is the depreciation rate of capital good j
- $\mathbb{E}(\boldsymbol{d}^j)$ is the expected return to capital good j.

Potential capital use $\bar{\boldsymbol{k}}$ is then constructed as a Törnqvist index in line with Knetsch (2013) from $\dot{\boldsymbol{k}}$ with the base year 1969 and an initial value of 100. The required return $\boldsymbol{r}$ derives from the zero-profit condition in Eq. (10), i.e., from an aggregate perspective, return to capital equals the capital share of output (here approximated by gross value added) over gross fixed capital (OECD 2009). The depreciation rate can be computed as volume of depreciation for capital good j in t over volume of net fixed assets of capital good j in t. Finally, as we assume rational agents with full information, we approximate expected returns (approximated by the the investment deflator) by the current trend growth rate.

II Total Factor Productivity

In this appendix, we discuss the prior assumptions and the outcomes of our estimation regarding total factor productivity (TFP).

We estimate TFP, obtained as the Solow residual, in natural logarithms, multiplied by 100. We drop the time-varying autoregressive coefficient from the baseline model. For our analysis, we generate 360,000 samples from the conditional posterior. To ensure our results are reliable, we discard the initial 10,000 samples as they may not yet represent the true distribution. To reduce autocorrelation and avoid redundancy, we keep only every seventh sample from the remaining pool.

We evaluate the performance of our sampling process to ensure its accuracy. We do this by means of Geweke t-tests and by examining integrated autocorrelation time (see e.g. the Appendix to Berger, Everaert, and Pozzi (2021) for a detailed description). These evaluations show that our sampling process has achieved good convergence, indicating that our results are stable and reliable. The full convergence results are available upon request.

II.1 Prior Distributions

Table 1 provides an overview of the prior information we used in the TFP (total factor productivity) model.

					quantiles	
Innovation variances			a	b	$\sqrt{\mathcal{Q}(0.01)}$	$\sqrt{\mathcal{Q}(0.99)}$
y_t^τ innovation variance	σ_τ^2	$\mathcal{IG}(a,b)$	40	0.01	0.013	0.019
y_t^g innovation variance	σ_g^2	$\mathcal{IG}(a,b)$	35	0.05	0.032	0.047
ψ_t^c innovation variance	$\sigma_{\psi^c}^2$	$\mathcal{IG}(a,b)$	5	4	0.587	1.768
Regression parameters					quantiles	
			μ	ξ	$\mathcal{Q}(0.01)$	$\mathcal{Q}(0.99)$
y_t^τ initial state	y_0^τ	calibrated	-693			
y_t^g initial state	y_0^g	$\mathcal{N}(\mu,\xi)$	1.5	0.15^2	1.151	1.849
ψ_t^c initial state	ψ_0^c	$\mathcal{N}(\mu,\xi)$	0	1^2	-2.326	2.326

Table 1 Prior distributions for relevant innovation variance and regression parameters of the total factor productivity model. $\mathcal{Q}(\cdot)$ denotes the quantile function.

We set the initial condition for TFP close to its actual observed value. For the innovation variances (essentially, how much TFP can change from one period to another), we use relatively detailed prior information in an inverse-gamma framework. This means we have a clear idea of how much we expect TFP to fluctuate over time that derives from the trend-cycle setup. When it comes to the initial estimate of TFP trend growth, we do not impose strong priors. Instead, we have moderately nonrestrictive prior information. This allows the model some flexibility in determining how TFP's trend may evolve.

II.2 Detailed Estimation and Projection Results

We estimate the baseline filter without the autoregressive component in the cycle and without bounding the trend component. Figures 1 depicts posterior results of all parameters associated with the TFP-specification. The upper panel of Figure 1 displays the TFP trend results, divided by 100.

Total factor productivity estimates and projections[1]

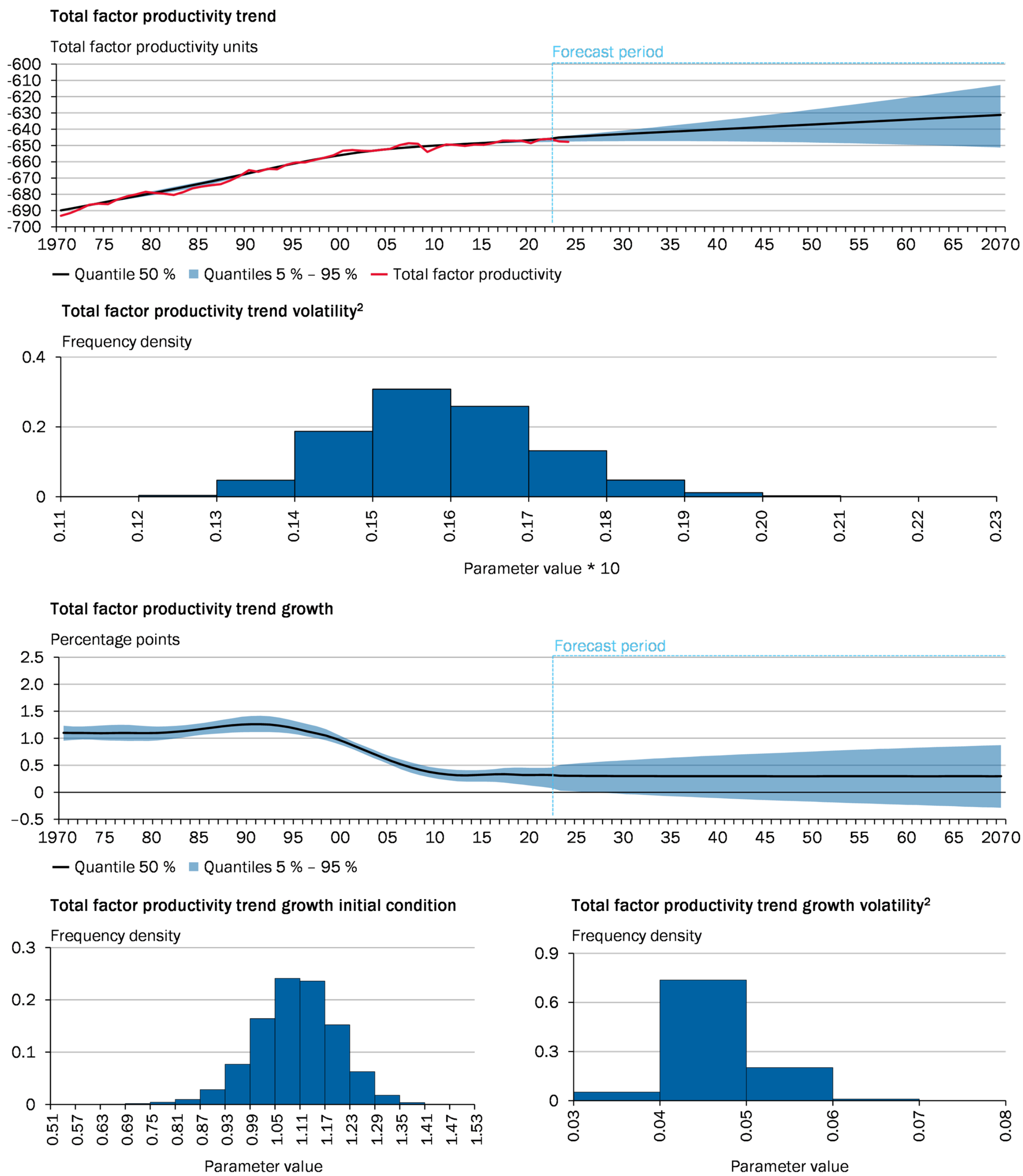

1 – Results are based on 50,000 retained posterior draws. Blue shaded area indicates 90 % probability mass. 2 – Computed as square root of inverse-gamma posterior.

Sources: Federal Statistical Office, IAB, OECD, own calculations

Figure 1 Trend component of total factor productivity (first row), its volatility (second row), trend growth (third row) and its initial condition and volatility (fourth row).

III Capital Stock

In this appendix, we will cover three key aspects related to capital use. First, we discuss the required rate of return. Then, we delve into investment and investment deflators. In addition, we provide details on our prior assumptions and the results of our estimation.

III.1 Required Rate of Return

The required rate of return (RRR) to capital derives from Eq. 10. In a first model, the 'core model' we decompose $(\mathbf{1}_T - \boldsymbol{\alpha})\boldsymbol{y}\boldsymbol{v}^{-1}$ into trend and cycle and in a second 'capital gain model', we filter $\boldsymbol{d}$. Note that the cyclical variation in $\boldsymbol{d}$ does not enter $\boldsymbol{r}$, as rational agents would not form their expectations based on cyclical variations in capital gains. That is, the cycle of $\boldsymbol{r}$ that ultimately gives rise to the cycle of capital use, is derived from cyclical variation in $(\mathbf{1}_T - \boldsymbol{\alpha})\boldsymbol{y}\boldsymbol{v}^{-1}$ alone. For both models, drop the time-varying autoregressive coefficient from the baseline specification.

For our analysis, we generate 360,000 samples from the conditional posterior. To ensure our results are reliable, we discard the initial 10,000 samples as they may not yet represent the true conditional posterior. To reduce autocorrelation and avoid redundancy, we keep only every seventh sample from the remaining pool. We evaluate the performance of our sampling process to ensure its accuracy. We do this by means of Geweke t-tests and by examining integrated autocorrelation time. These evaluations show that our sampling process has achieved good convergence, indicating that our results are stable and reliable. The full convergence results are available upon request.

III.1.1 Prior Distributions

Table 2 summarizes information on the prior distributions for both the 'core model' and the 'capital gain model'.

We set the initial conditions for both trends close to their actual observed values. We use relatively detailed prior information for the innovation variances and trend growth. For the remaining priors (which cover various aspects of the model), we adopt relatively uninformative priors. The core component model is estimated in logarithms multiplied by 100.

For our analysis, we generate 360,000 samples from the conditional posterior. To ensure our results are reliable, we discard the initial 10,000 samples as they may not yet represent the true distribution. To reduce autocorrelation and avoid redundancy, we keep only every seventh sample from the remaining pool.

Innovation variances						
					quantiles	
			a	b	$\sqrt{\mathcal{Q}(0.01)}$	$\sqrt{\mathcal{Q}(0.99)}$
core model						
y_t^τ innovation variance	σ_τ^2	$\mathcal{IG}\,(a,b)$	50	1	0.121	0.169
y_t^g innovation variance	σ_g^2	$\mathcal{IG}\,(a,b)$	50	2	0.172	0.239
ψ_t^c innovation variance	$\sigma_{\psi^c}^2$	$\mathcal{IG}\,(a,b)$	5	4	0.587	1.768
capital gains model						
y_t^τ innovation variance	σ_τ^2	$\mathcal{IG}\,(a,b)$	140	0.01^2	0.001	0.001
y_t^g innovation variance	σ_g^2	$\mathcal{IG}\,(a,b)$	130	0.1	0.025	0.031
ψ_t^c innovation variance	$\sigma_{\psi^c}^2$	$\mathcal{IG}\,(a,b)$	5	4	0.587	1.768

Regression parameters						
					quantiles	
			μ	ξ	$\mathcal{Q}(0.01)$	$\mathcal{Q}(0.99)$
core model						
y_t^τ initial state	y_0^τ	calibrated	201.49			
y_t^g AR(1)	y_0^g	$\mathcal{N}\,(\mu,\xi)$	0.95	0.1^2	0.704	0.998
ψ_t^c initial state	ψ_0^c	$\mathcal{N}\,(\mu,\xi)$	0	2^2	-4.653	4.653
capital gains model						
y_t^τ initial state	y_0^τ	calibrated	28			
y_t^g initial state	y_0^g	$\mathcal{N}\,(\mu,\xi)$	2.47	0.01^2	2.457	2.503
ψ_t^c initial state	ψ_0^c	$\mathcal{N}\,(\mu,\xi)$	0	2^2	-4.653	4.653

Table 2 Prior distributions for relevant innovation variance and regression parameters of the required rate of return models. $\mathcal{Q}(\cdot)$ denotes the quantile function.

III.1.2 Detailed Estimation and Projection Results

We estimate the baseline filter without the autoregressive component in the cycle and without bounding the trend component. Figures 2 shows the outcomes related to all the parameters in the core required rate of return specification. Figures 3 provides similar insights but for the capital gain model.

Required rate of return to capital – core component estimates and projections[1]

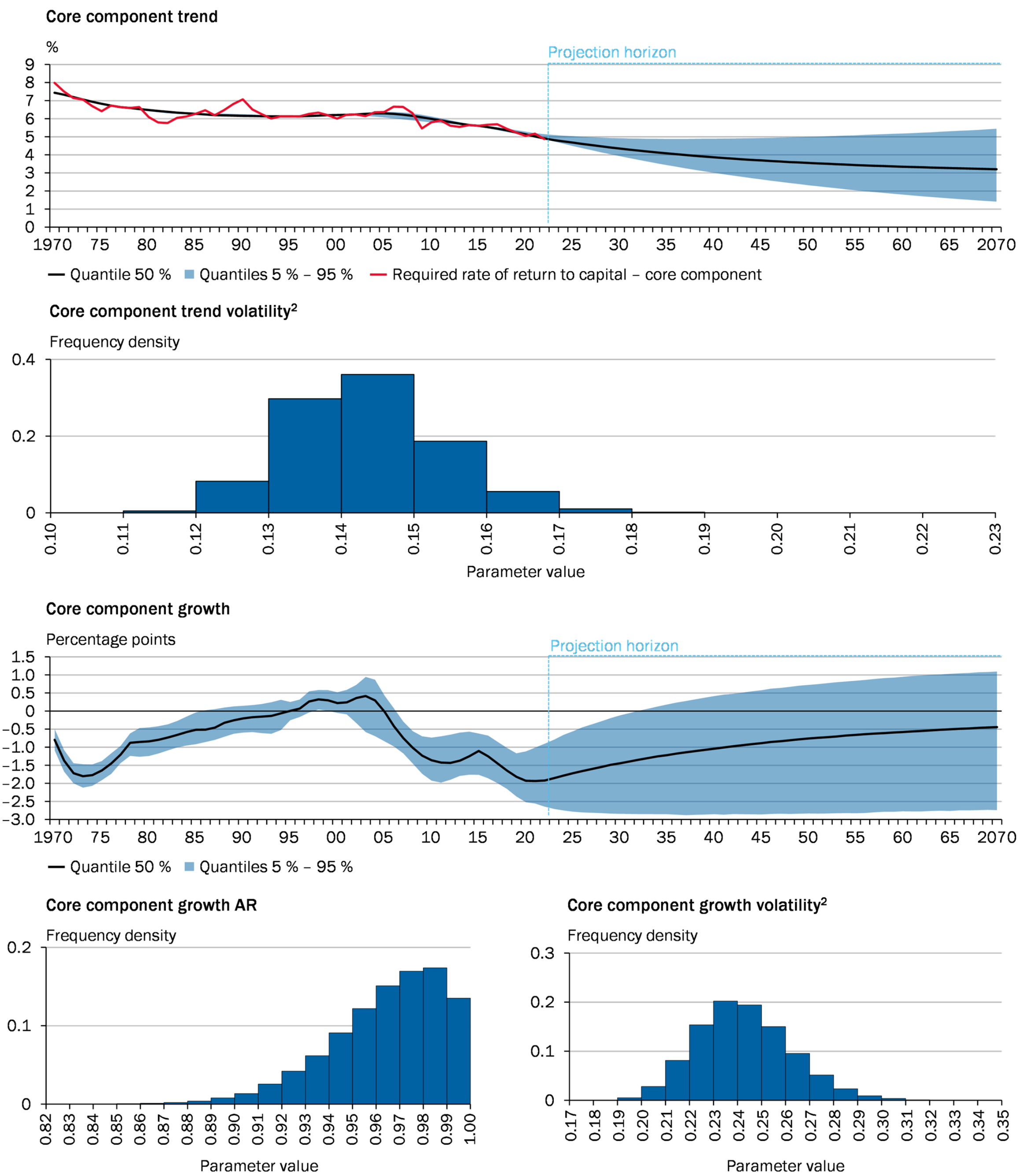

1 – Results are based on 50,000 retained posterior draws. Blue shaded area indicates 90 % probability mass. 2 – Computed as square root of inverse-gamma posterior.

Sources: Federal Statistical Office, own calculations

Figure 2 Trend component of the core component of the required rate of return (first row), its volatility (second row), trend growth (third row) and its initial condition and volatility (fourth row).

Required rate of return to capital – capital gains component estimates and projections[1]

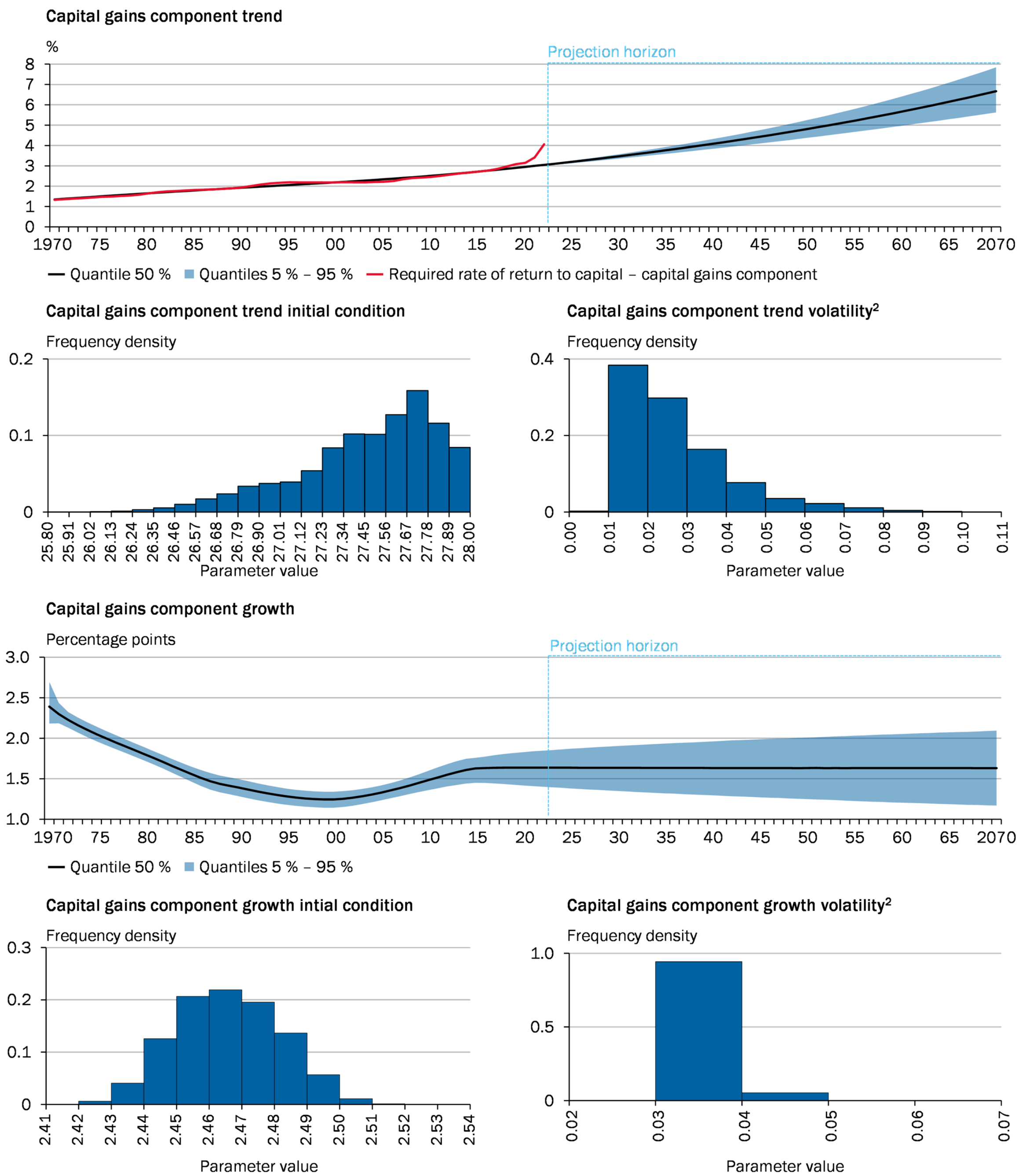

1 – Results are based on 50,000 retained posterior draws. Blue shaded area indicates 90 % probability mass. 2 – Computed as square root of inverse-gamma posterior.

Sources: Federal Statistical Office, own calculations

Figure 3 Trend component of the capital gains component of the required rate of return (first row), its volatility (second row), trend growth (third row) and its initial condition and volatility (fourth row).

III.2 Investment

In this appendix, we present detailed results related to real investment. Specifically, we look at real investment levels of chained volumes, where the base year is 2015. Investment is crucial to compute real additions to capital, $\boldsymbol{v}^{+j}$ as real investment in time t weighted by the ratio of nominal investment and nominal gross fixed assets in time $t-1$. Before conducting our analysis, we made a transformation to the investment data. We converted all the real investment series into natural logarithms and then scaled the values by multiplying them by 100. We drop the time-varying autoregressive coefficient from the baseline model.

For our analysis, we generate 360,000 samples from the conditional posterior. To ensure our results are reliable, we discard the initial 10,000 samples as they may not yet represent the true distribution. To reduce autocorrelation and avoid redundancy, we keep only every seventh sample from the remaining pool. We evaluate the performance of our sampling process to ensure its accuracy. We do this by means of Geweke t-tests and by examining integrated autocorrelation time. These evaluations show that our sampling process has achieved good convergence, indicating that our results are stable and reliable. The full convergence results are available upon request.

III.2.1 Prior Distribution

Tables 3 and 4 summarize information on the prior distributions for all real investment models.

Innovation variances						
					quantiles	
			a	b	$\sqrt{\mathcal{Q}(0.01)}$	$\sqrt{\mathcal{Q}(0.99)}$
equipment capital						
y_t^τ innovation variance	σ_τ^2	$\mathcal{IG}(a,b)$	80	0.1	0.031	0.041
y_t^g innovation variance	σ_g^2	$\mathcal{IG}(a,b)$	80	1.5	0.121	0.157
ψ_t^c innovation variance	$\sigma_{\psi^c}^2$	$\mathcal{IG}(a,b)$	5	4	0.587	1.768
residential capital						
y_t^τ innovation variance	σ_τ^2	$\mathcal{IG}(a,b)$	80	0.1	0.031	0.041
y_t^g innovation variance	σ_g^2	$\mathcal{IG}(a,b)$	60	1.5	0.137	0.186
ψ_t^c innovation variance	$\sigma_{\psi^c}^2$	$\mathcal{IG}(a,b)$	5	4	0.587	1.768
nonresidential capital						
y_t^τ innovation variance	σ_τ^2	$\mathcal{IG}(a,b)$	80	2	0.140	0.182
y_t^g innovation variance	σ_g^2	$\mathcal{IG}(a,b)$	80	2	0.140	0.182
ψ_t^c innovation variance	$\sigma_{\psi^c}^2$	$\mathcal{IG}(a,b)$	5	4	0.587	1.768
other capital						
y_t^τ innovation variance	σ_τ^2	$\mathcal{IG}(a,b)$	80	0.001	0.003	0.004
y_t^g innovation variance	σ_g^2	$\mathcal{IG}(a,b)$	70	0.01	0.010	0.013
ψ_t^c innovation variance	$\sigma_{\psi^c}^2$	$\mathcal{IG}(a,b)$	5	4	0.587	1.768

Table 3 Prior distributions for relevant innovation variance and regression parameters of the investment models. $\mathcal{Q}(\cdot)$ denotes the quantile function.

Regression parameters						
					quantiles	
			μ	ξ	$\mathcal{Q}(0.01)$	$\mathcal{Q}(0.99)$
equipment capital						
y_t^τ initial state	y_0^τ	calibrated	435.4			
y_t^g initial state	y_0^g	$\mathcal{N}(\mu, \xi)$	0	1^2	-2.326	2.326
ψ_t^c initial state	ψ_0^c	$\mathcal{N}(\mu, \xi)$	0	2^2	-4.653	4.653
residential capital						
y_t^τ initial state	y_0^τ	calibrated	471.9			
y_t^g initial state	y_0^g	$\mathcal{N}(\mu, \xi)$	0	1^2	-2.326	2.326
ψ_t^c initial state	ψ_0^c	$\mathcal{N}(\mu, \xi)$	0	2^2	-4.653	4.653
nonresidential capital						
y_t^τ initial state	y_0^τ	calibrated	485			
y_t^g initial state	y_0^g	$\mathcal{N}(\mu, \xi)$	1	0.25^2	0.418	1.582
ψ_t^c initial state	ψ_0^c	$\mathcal{N}(\mu, \xi)$	0	2^2	-4.653	4.653
other capital						
y_t^τ initial state	y_0^τ	calibrated	192.45			
y_t^g initial state	y_0^g	$\mathcal{N}(\mu, \xi)$	15.5	1		
ψ_t^c initial state	ψ_0^c	$\mathcal{N}(\mu, \xi)$	0	2^2	-4.653	4.653

Table 4 Prior distributions for relevant innovation variance and regression parameters of the total factor productivity model. $\mathcal{Q}(\cdot)$ denotes the quantile function.

III.2.2 Detailed Estimation and Projection Results

In the following, we present detailed estimation results.

- Figures 4 presents detailed estimation and projection results for real investment into equipment.
- Figures 5 presents detailed estimation and projection results for real investment into residential capital.
- Figures 6 presents detailed estimation and projection results for real investment into nonresidential capital.
- Figures 7 presents detailed estimation and projection results for real investment into other capital.

Equipment capital investment estimates and projections[1]

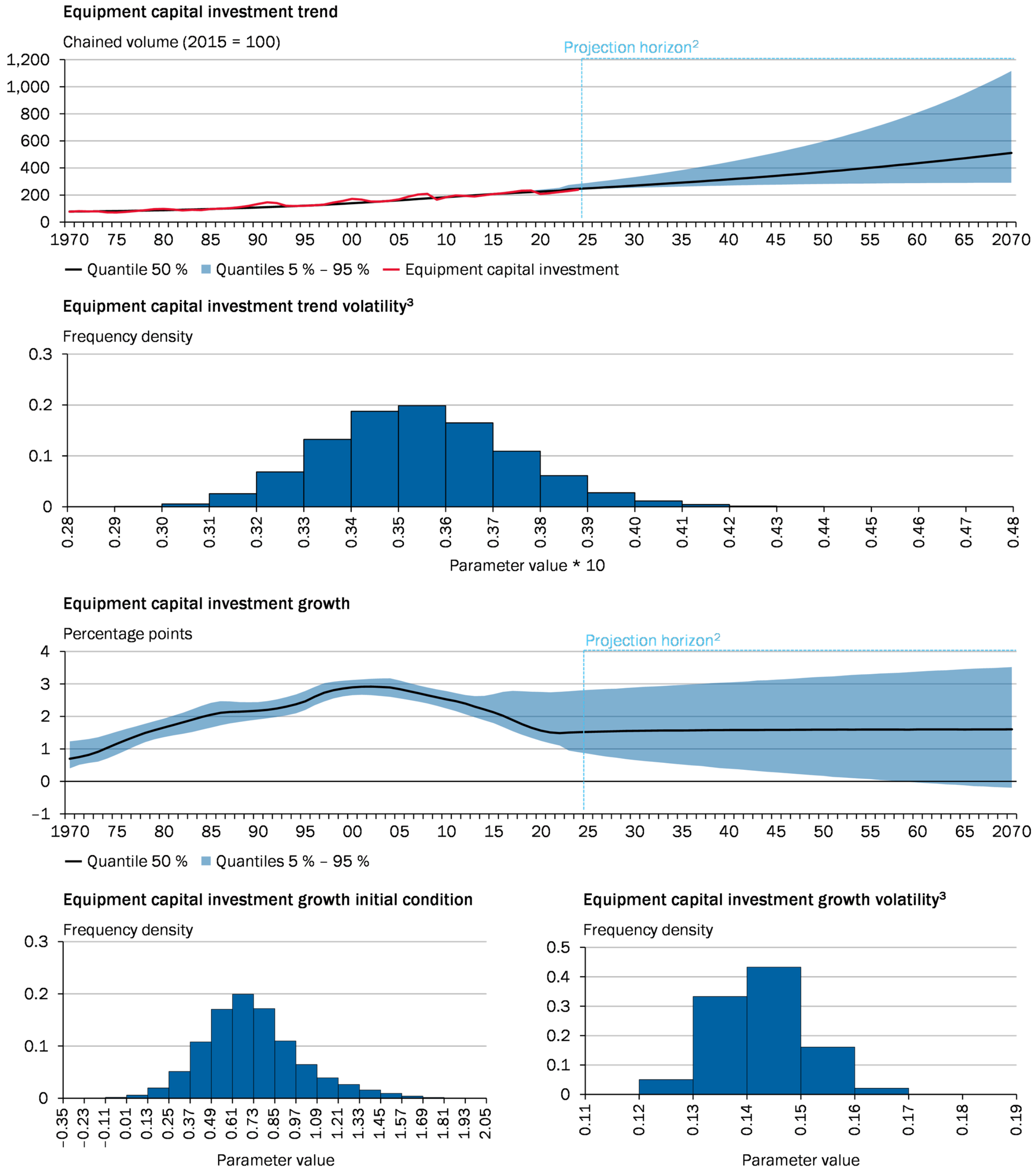

1 – Results are based on 50,000 retained posterior draws. Blue shaded area indicates 90 % probability mass. 2 – Projection horizon is 2025–2070. For 2023 and 2024, we use the GCEE short-run business cycle forecasts and treat them as data. 3 – Computed as square root of inverse-gamma posterior.

Sources: Federal Statistical Office, own calculations

Figure 4 Trend component of real investment into equipment capital (first row), its volatility (second row), trend growth (third row) and its initial condition and volatility (fourth row).

Residential capital investment estimates and projections[1]

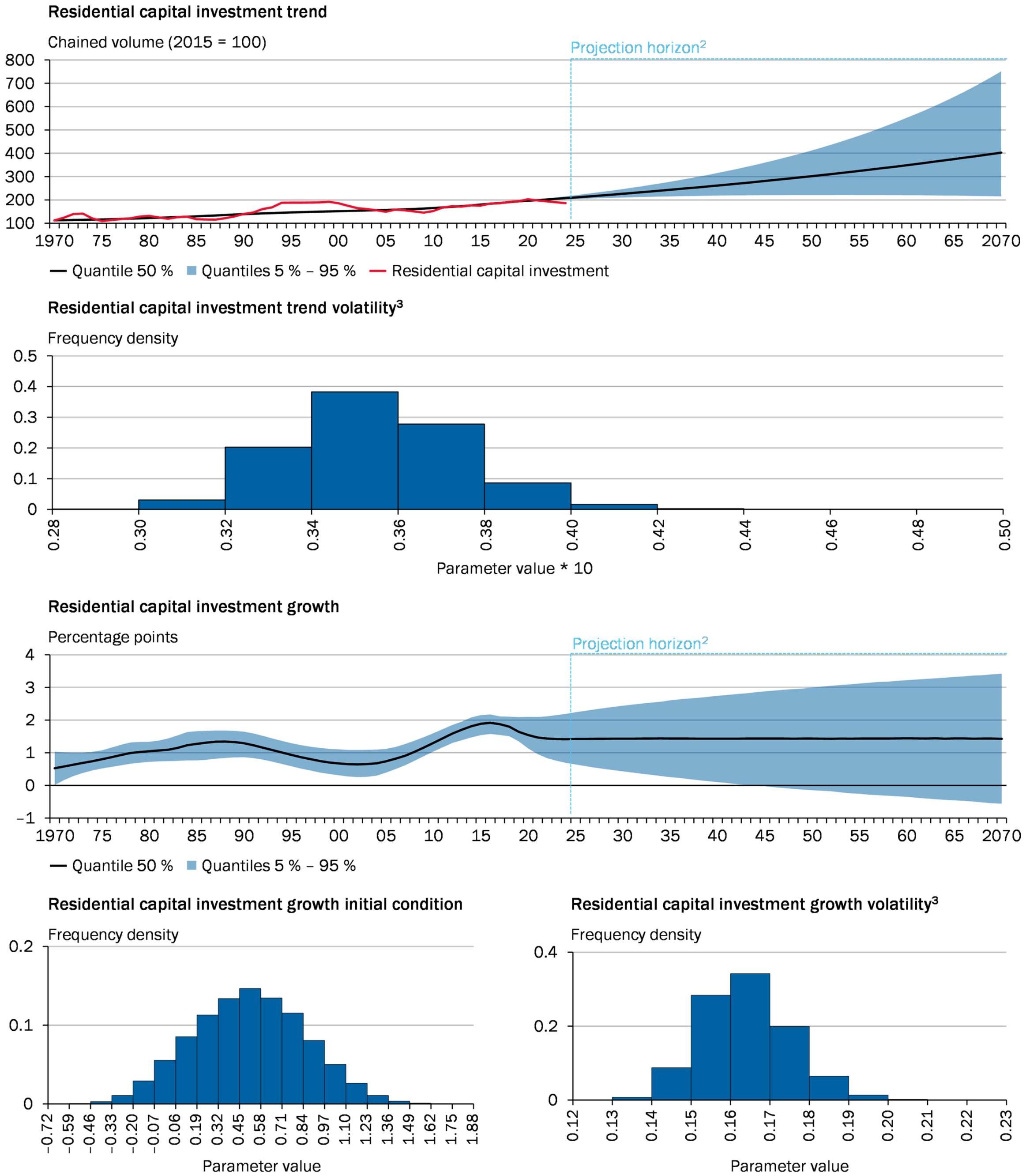

1 – Results are based on 50,000 retained posterior draws. Blue shaded area indicates 90 % probability mass. 2 – Projection horizon is 2025–2070. For 2023 and 2024, we use the GCEE short-run business cycle forecasts and treat them as data. 3 – Computed as square root of inverse-gamma posterior.

Sources: Federal Statistical Office, own calculations

Figure 5 Trend component of real investment into residential capital (first row), its volatility (second row), trend growth (third row) and its initial condition and volatility (fourth row).

Non-residential capital investment estimates and projections[1]

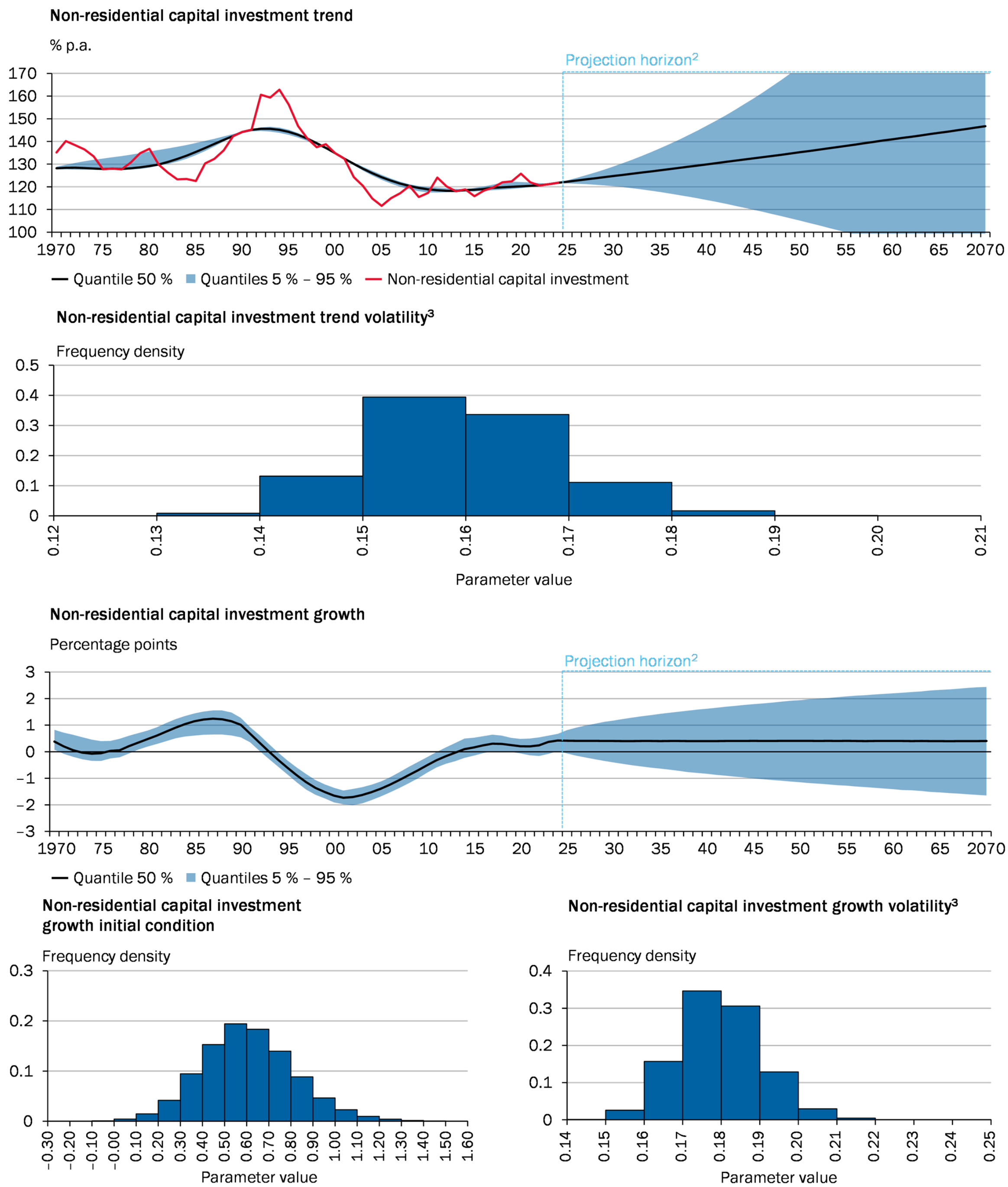

1 – Results are based on 50,000 retained posterior draws. Blue shaded area indicates 90 % probability mass. 2 – Projection horizon is 2025–2070. For 2023 and 2024, we use the GCEE short-run business cycle forecasts and treat them as data. 3 – Computed as square root of inverse-gamma posterior.

Sources: Federal Statistical Office, own calculations

Figure 6 Trend component of real investment into nonresidential capital (first row), its volatility (second row), trend growth (third row) and its initial condition and volatility (fourth row).

Other capital investment estimates and projections[1]

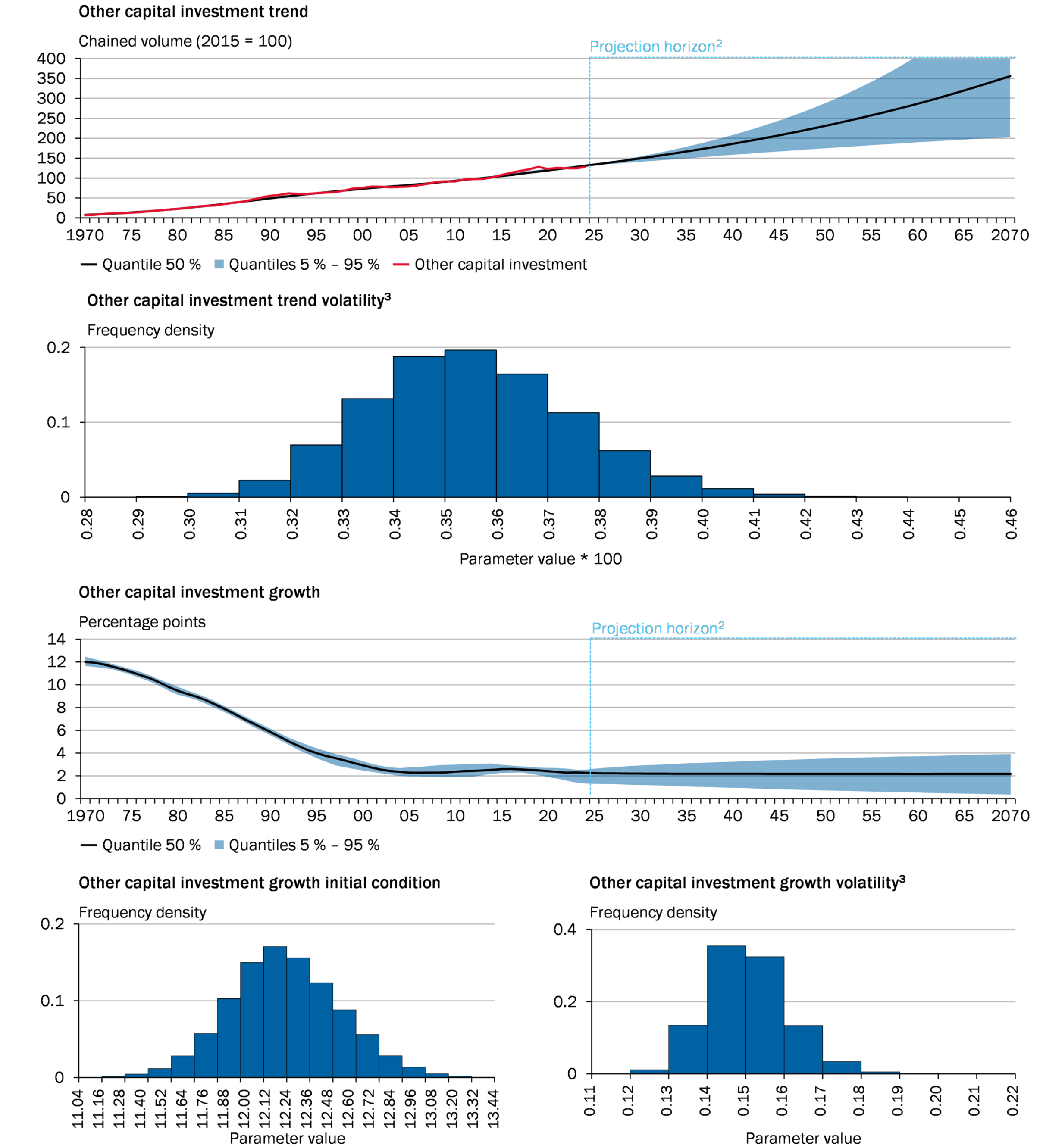

1 – Results are based on 50,000 retained posterior draws. Blue shaded area indicates 90 % probability mass. 2 – Projection horizon is 2025–2070. For 2023 and 2024, we use the GCEE short-run business cycle forecasts and treat them as data. 3 – Computed as square root of inverse-gamma posterior.

Sources: Federal Statistical Office, own calculations

Figure 7 Trend component of real investment into other capital (first row), its volatility (second row), trend growth (third row) and its initial condition and volatility (fourth row).

III.3 Investment Deflator

In this appendix, we present detailed estimation and prior specification results related to investment deflators. Investment deflators are essential because they are used as expectations for capital gains in the capital cost equation. They help us anticipate the changes in the value of capital assets over time. These deflators are expressed in logarithmic form and are based on chained volumes, where the reference year is 2015. We drop the time-varying autoregressive coefficient from the baseline model.

For our analysis, we generate 360,000 samples from the conditional posterior. To ensure our results are reliable, we discard the initial 10,000 samples as they may not yet represent the true distribution. To reduce autocorrelation and avoid redundancy, we keep only every seventh sample from the remaining pool. We evaluate the performance of our sampling process to ensure its accuracy. We do this by means of Geweke t-tests and by examining integrated autocorrelation time. These evaluations show that our sampling process has achieved good convergence, indicating that our results are stable and reliable. The full convergence results are available upon request.

III.3.1 Prior Distribution

Tables 5 and 6 show the priors for innovation variance and regression parameters, respectively.

Innovation variances						
					quantiles	
			a	b	$\sqrt{\mathcal{Q}(0.01)}$	$\sqrt{\mathcal{Q}(0.99)}$
equipment capital						
y_t^τ innovation variance	σ_τ^2	$\mathcal{IG}\,(a,b)$	90	0.1^2	0.003	0.004
y_t^g innovation variance	σ_g^2	$\mathcal{IG}\,(a,b)$	50	0.01^2	0.004	0.005
ψ_t^c innovation variance	$\sigma_{\psi^c}^2$	$\mathcal{IG}\,(a,b)$	5	4	0.587	1.768
residential capital						
y_t^τ innovation variance	σ_τ^2	$\mathcal{IG}\,(a,b)$	90	0.1	0.030	0.038
y_t^g innovation variance	σ_g^2	$\mathcal{IG}\,(a,b)$	90	0.15	0.036	0.046
ψ_t^c innovation variance	$\sigma_{\psi^c}^2$	$\mathcal{IG}\,(a,b)$	5	4	0.587	1.768
nonresidential capital						
y_t^τ innovation variance	σ_τ^2	$\mathcal{IG}\,(a,b)$	80	0.1	0.031	0.041
y_t^g innovation variance	σ_g^2	$\mathcal{IG}\,(a,b)$	80	0.5	0.070	0.091
ψ_t^c innovation variance	$\sigma_{\psi^c}^2$	$\mathcal{IG}\,(a,b)$	5	4	0.587	1.768
other capital						
y_t^τ innovation variance	σ_τ^2	$\mathcal{IG}\,(a,b)$	80	0.1^2	0.010	0.013
y_t^g innovation variance	σ_g^2	$\mathcal{IG}\,(a,b)$	70	0.1	0.033	0.044
ψ_t^c innovation variance	$\sigma_{\psi^c}^2$	$\mathcal{IG}\,(a,b)$	5	4	0.587	1.768

Table 5 Prior distributions for relevant innovation variance parameters of the investment deflator models. $\mathcal{Q}(\cdot)$ denotes the quantile function.

Regression parameters							
						quantiles	
				μ	ξ	$\mathcal{Q}(0.01)$	$\mathcal{Q}(0.99)$
equipment capital							
y_t^τ	initial state	y_0^τ	calibrated	399.49			
y_t^g	initial state	y_0^g	$\mathcal{N}(\mu, \xi)$	4.67	1^2	2.344	6.996
ψ_t^c	initial state	ψ_0^c	$\mathcal{N}(\mu, \xi)$	0	2^2	-4.653	4.653
residential capital							
y_t^τ	initial state	y_0^τ	calibrated	318.57			
y_t^g	initial state	y_0^g	$\mathcal{N}(\mu, \xi)$	9.43	1^2	7.104	11.756
ψ_t^c	initial state	ψ_0^c	$\mathcal{N}(\mu, \xi)$	0	2^2	-4.653	4.653
nonresidential capital							
y_t^τ	initial state	y_0^τ	calibrated	335.92			
y_t^g	initial state	y_0^g	$\mathcal{N}(\mu, \xi)$	7.88	1^2	5.554	10.206
ψ_t^c	initial state	ψ_0^c	$\mathcal{N}(\mu, \xi)$	0	2^2	-4.653	4.653
other capital							
y_t^τ	initial state	y_0^τ	calibrated	429.21			
y_t^g	initial state	y_0^g	$\mathcal{N}(\mu, \xi)$	0.68	1^2	-1.646	3.006
ψ_t^c	initial state	ψ_0^c	$\mathcal{N}(\mu, \xi)$	0	2^2	-4.653	4.653

Table 6 Prior distributions for relevant innovation variance and regression parameters of the investment deflator models. $\mathcal{Q}(\cdot)$ denotes the quantile function.

III.3.2 Detailed Estimation and Projection Results

In the following, we present detailed estimation results.

- Figures 8 presents detailed estimation and projection results for the equipment capital deflator.
- Figures 9 presents detailed estimation and projection results for the residential capital deflator.
- Figures 10 presents detailed estimation and projection results for the nonresidential capital deflator.
- Figures 11 presents detailed estimation and projection results for the other capital deflator.

Equipment capital investment deflator estimates and projections[1]

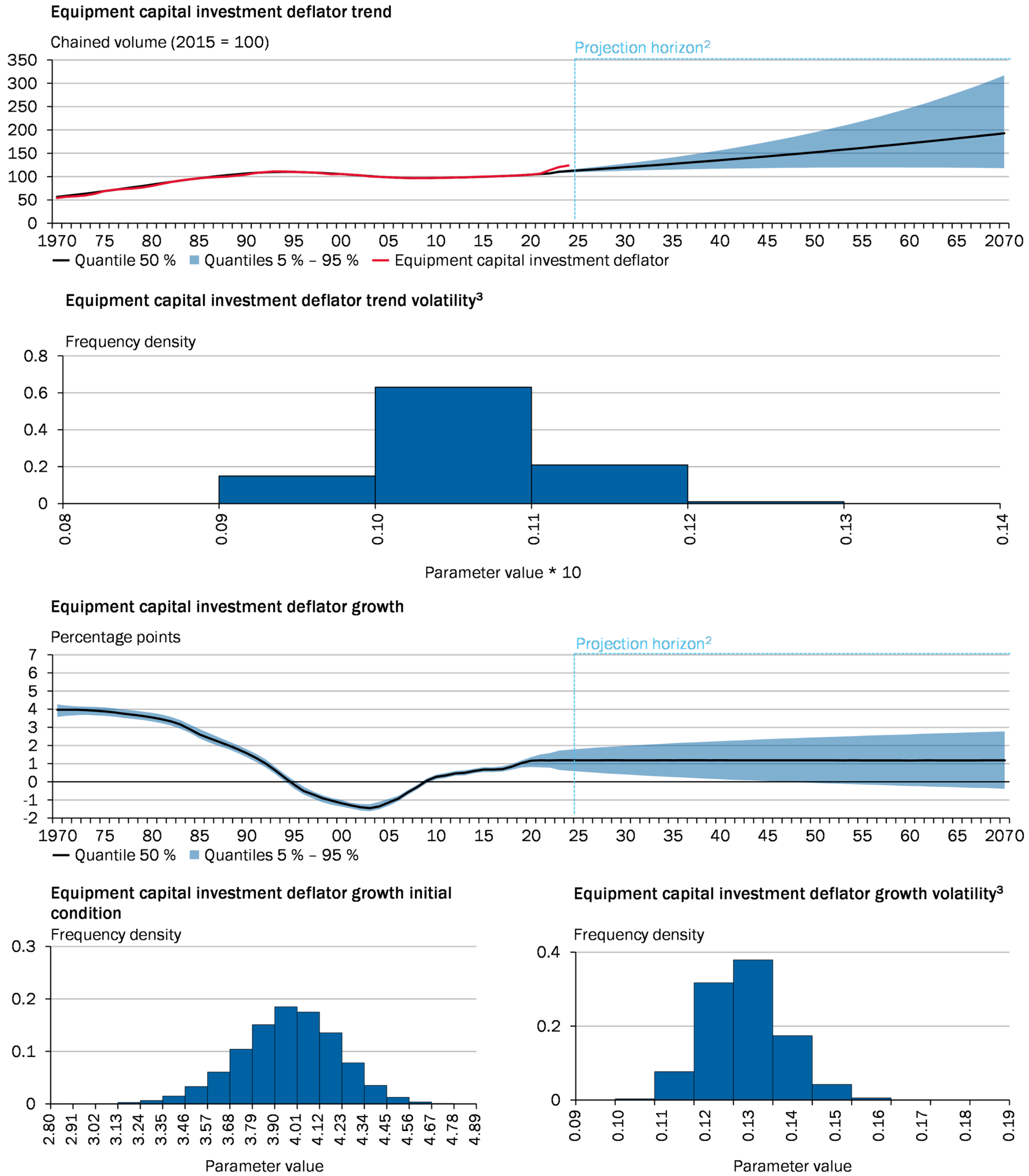

1 – Results are based on 50,000 retained posterior draws. Blue shaded area indicates 90 % probability mass. 2 – Projection horizon is 2025–2070. For 2023 and 2024, we use the GCEE short-run business cycle forecasts and treat them as data. 3 – Computed as square root of inverse-gamma posterior.

Sources: Federal Statistical Office, own calculations

Figure 8 Trend component of deflator of investment into equipment capital (first row), its volatility (second row), trend growth (third row) and its initial condition and volatility (fourth row).

Residential capital investment deflator estimates and projections[1]

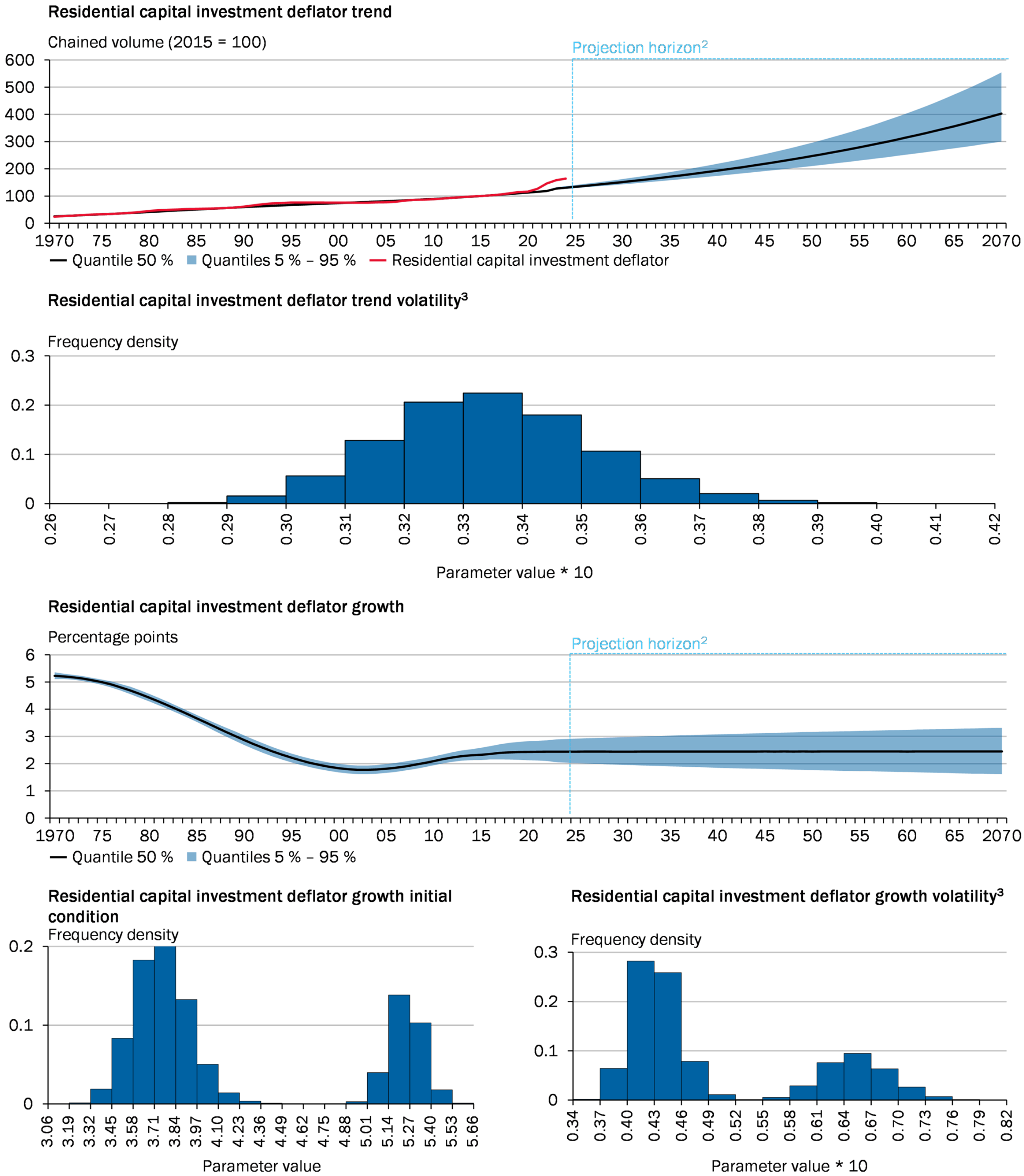

1 – Results are based on 50,000 retained posterior draws. Blue shaded area indicates 90 % probability mass. 2 – Projection horizon is 2025–2070. For 2023 and 2024, we use the GCEE short-run business cycle forecasts and treat them as data. 3 – Computed as square root of inverse-gamma posterior.

Sources: Federal Statistical Office, own calculations

Figure 9 Trend component of deflator of investment into residential capital (first row), its volatility (second row), trend growth (third row) and its initial condition and volatility (fourth row).

Non-residential capital investment deflator estimates and projections[1]

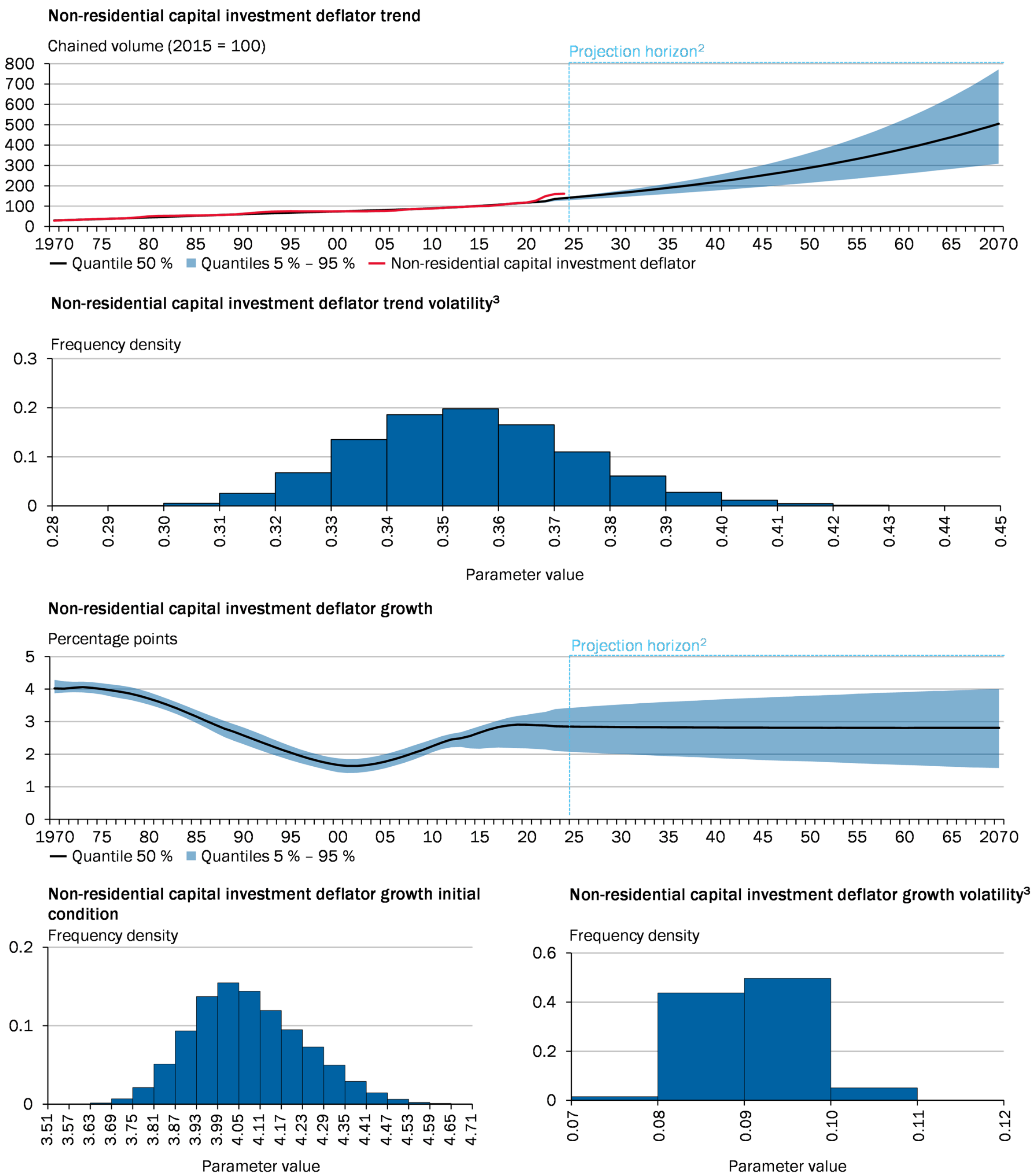

1 – Results are based on 50,000 retained posterior draws. Blue shaded area indicates 90 % probability mass. 2 – Projection horizon is 2025–2070. For 2023 and 2024, we use the GCEE short-run business cycle forecasts and treat them as data. 3 – Computed as square root of inverse-gamma posterior.

Sources: Federal Statistical Office, own calculations

Figure 10 Trend component of deflator of investment into nonresidential capital (first row), its volatility (second row), trend growth (third row) and its initial condition and volatility (fourth row).

Other capital investment deflator estimates and projections[1]

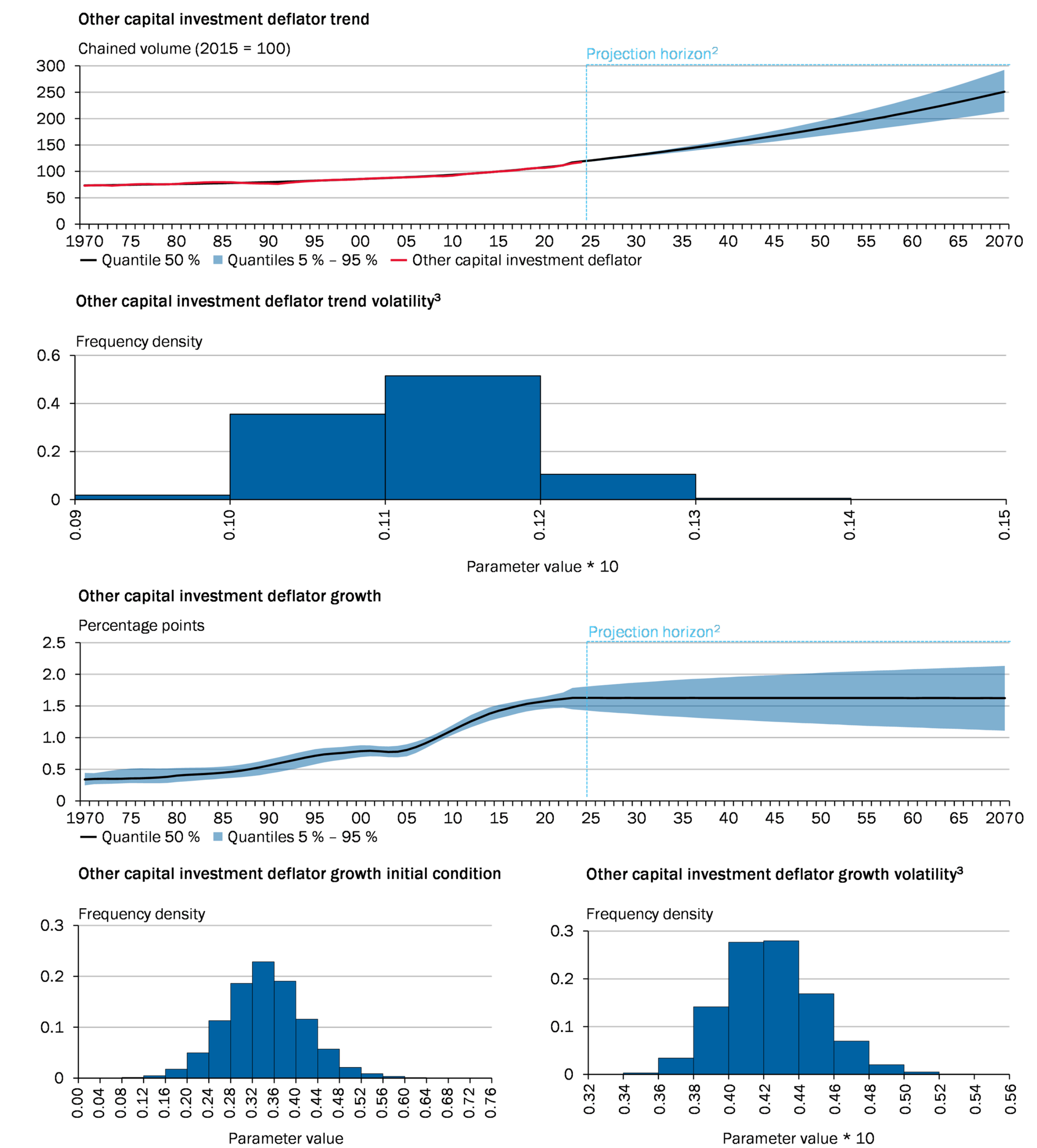

1 – Results are based on 50,000 retained posterior draws. Blue shaded area indicates 90 % probability mass. 2 – Projection horizon is 2025–2070. For 2023 and 2024, we use the GCEE short-run business cycle forecasts and treat them as data. 3 – Computed as square root of inverse-gamma posterior.

Sources: Federal Statistical Office, own calculations

Figure 11 Trend component of deflator of investment into other capital (first row), its volatility (second row), trend growth (third row) and its initial condition and volatility (fourth row).

IV Labor

This appendix presents detailed prior specification and estimation results for hours worked (Appendix IV.1), the natural rate of unemployment (Appendix IV.2), and participation rates (Appendix IV.3). The components aggregate as shown in Eq. 2.

IV.1 Hours

This appendix provides a detailed account of the prior specifications and estimation outcomes related to hours. It is important to note that all trends are bounded from zero and above. Differing from the baseline filter, we employ an autoregressive AR(1) specification for trend growth with the exception of aggregate historical hours (1970–1990). The autoregressive coefficient is readily sampled using the Metropolis-Hastings algorithm introduced by Chib and Greenberg (1994). This choice prevents components with negative trend growth from approaching the lower bound in the limit. Before commencing our analysis, we applied a data transformation to the hours data set. This transformation involved converting all series with the exception of aggregate historical hours (1970–1990) into their natural logarithms and subsequently scaling the values by a factor of 100. Dis-aggregated information in the spirit of Eq. 4 is only available after the year 1991. Therefore, we filter total hours for the period of 1970 − 1990 and hours for full-time, part-time and self-employed workers as well as part-time and self-employment rates after 1991.

IV.1.1 Prior Distributions

In Tables 7 and 8, we have assembled a set of parameter values that define our prior distributions. To conduct our analysis, we generated a total of 360,000 samples from the conditional posterior. To ensure the reliability of our results, we decided to discard the initial 10,000 samples as they may not yet accurately represent the true distribution. Concerning the part-time and self-employment rates, we obtained 101,000 draws from the conditional posterior distribution and discarded the initial 1,000 draws. From the remaining pool of samples, we retained only every seventh sample. We took this step to reduce autocorrelation and avoid unnecessary redundancy in our results. Our sampling method's convergence was rigorously assessed through various diagnostic tests, including Geweke t-tests and integrated autocorrelation times. The results from these tests provided strong evidence that our sampler had achieved a satisfactory level of convergence. Furthermore, the examination of trace plots yielded similar insights into the convergence of our model.

Regression parameters							
						quantiles	
				μ	ξ	$\mathcal{Q}(0.01)$	$\mathcal{Q}(0.99)$
part-time rate							
y_t^τ initial state		y_0^τ	calibrated	18.51			
self-employment rate							
y_t^τ initial state		y_0^τ	calibrated	9.17			
aggregate hours 1970–1990							
y_t^τ initial state		y_0^τ	calibrated	757.93			
full-time hours							
y_t^τ initial state		y_0^τ	calibrated	740.21			
part-time hours							
y_t^τ initial state		y_0^τ	calibrated	664.98			
self-employed hours							
y_t^τ initial state		y_0^τ	calibrated	774.01			
all hours							
ψ_t^c initial state		ψ_0^c	$\mathcal{N}(\mu, \xi)$	0	2^2	-4.653	4.653
all models							
y_t^g AR(1)		ϕ^g	$\mathcal{N}(\mu, \xi)$	0	1^2	-2.326	2.326

Trend bounds			
all hours			
			parameter value
y^τ	upper trend bound	$\overline{y^\tau}$	∞
y^τ	lower trend bound	$\underline{y^\tau}$	0
all rates			
y^τ	upper trend bound	$\overline{y^\tau}$	100
y^τ	lower trend bound	$\underline{y^\tau}$	0
all models			
ϕ^g	upper AR bound	$\overline{\phi^g}$	1
ϕ^g	lower AR bound	$\underline{\phi^g}$	-1

Table 7 Prior distributions for relevant innovation variance and regression parameters of hours as well as self-employment and part-time rates. $\mathcal{Q}(\cdot)$ denotes the quantile function. The initial state for historical aggregate hours has the same prior as the AR(1) coefficient for the remainder of the models.

Innovation variances for rates						
					quantiles	
			a	b	$\sqrt{\mathcal{Q}(0.01)}$	$\sqrt{\mathcal{Q}(0.99)}$
rates						
y_t^τ innovation variance	σ_τ^2	$\mathcal{IG}\,(a.b)$	20	1	0.177	0.300
y_t^g innovation variance	σ_g^2	$\mathcal{IG}\,(a.b)$	20	0.5	0.125	0.212
hours						
y_t^τ innovation variance	σ_τ^2	$\mathcal{IG}\,(a.b)$	30	0.09	0.045	0.069
y_t^g innovation variance	σ_g^2	$\mathcal{IG}\,(a.b)$	25	0.45	0.109	0.174
ψ_t^c innovation variance	$\sigma_{\psi^c}^2$	$\mathcal{IG}\,(a,b)$	5	4	0.587	1.768

Table 8 Prior distributions for relevant innovation variance and regression parameters of hours as well as self-employment and part-time rates. $\mathcal{Q}(\cdot)$ denotes the quantile function.

IV.1.2 Detailed Estimation and Projection Results

In the following, we present detailed estimation results.

- Figures 12 presents detailed estimation and projection results for total hours for the period of 1970 – 1990.
- Figures 13 presents detailed estimation and projection results for full-time hours since 1991.
- Figures 14 presents detailed estimation and projection results for part-time hours since 1991.
- Figures 15 presents detailed estimation and projection results for self-employment hours since 1991.
- Figure 16 presents detailed estimation and projection results for the self-employment rate since 1991.
- Figure 17 presents detailed estimation and projection results for part-time rate since 1991.

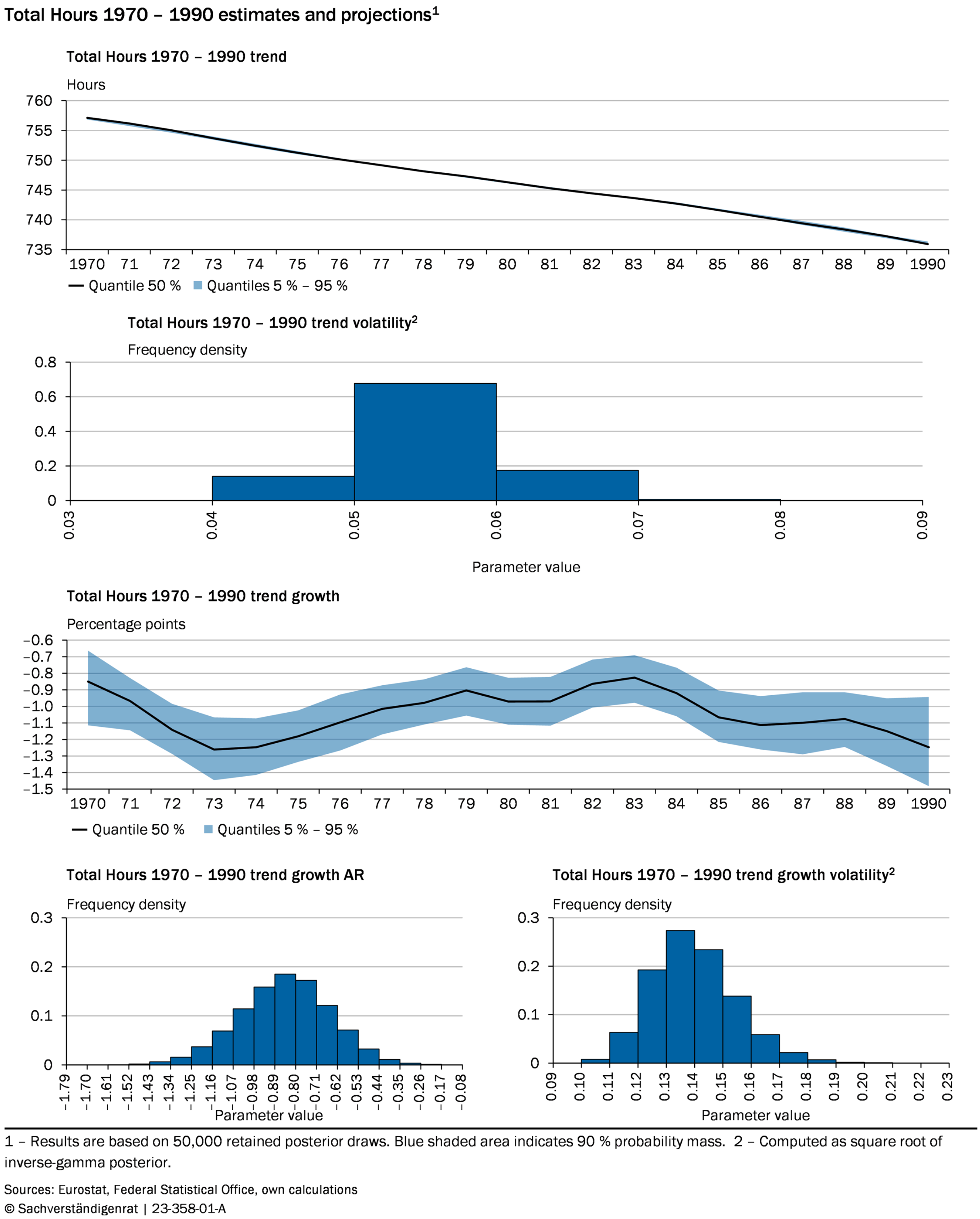

Figure 12 Trend component of total hours 1970 – 1991 (first row), its volatility (second row), trend growth (third row) and its autoregressive parameters and volatility (fourth row).

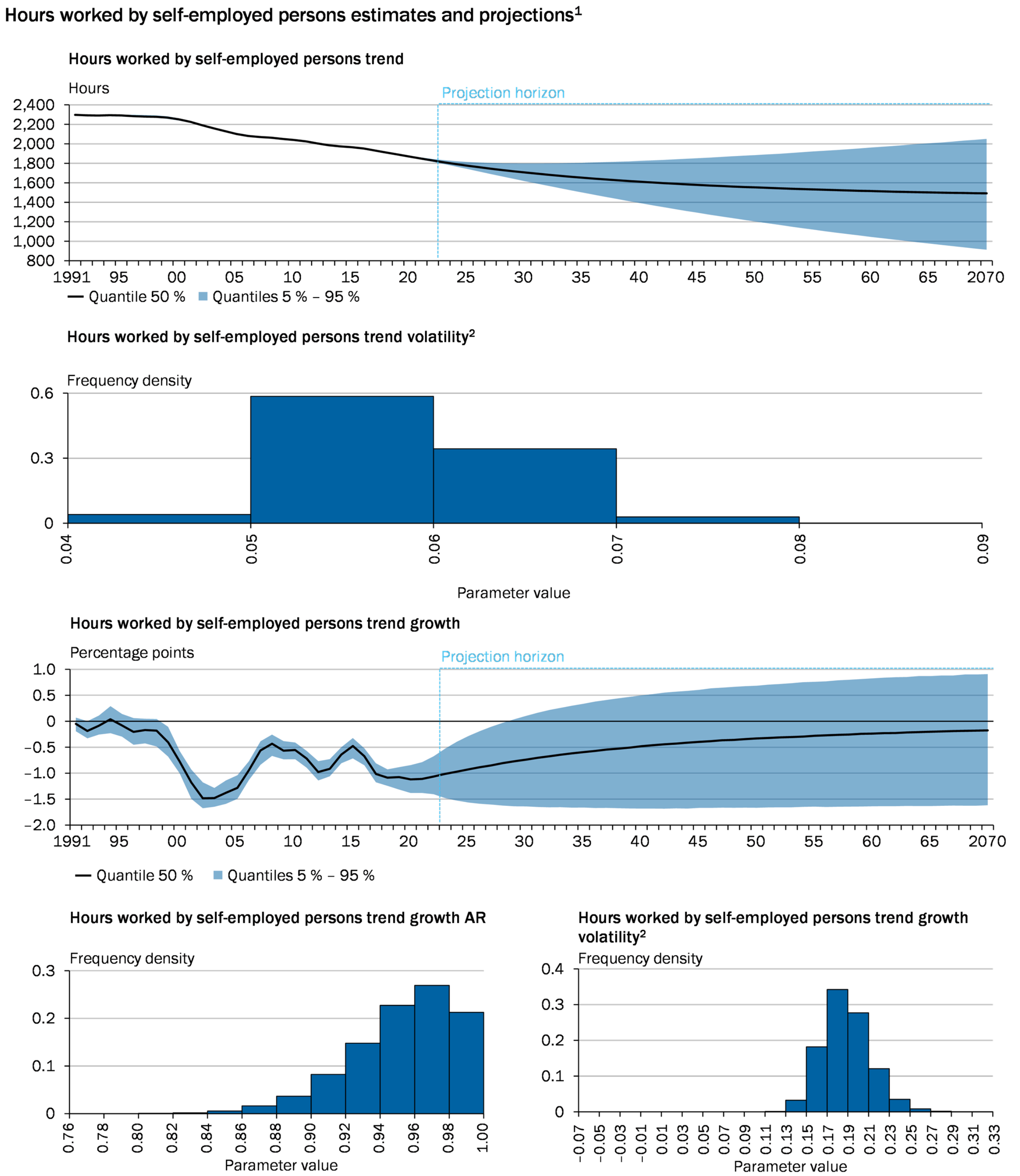

1 – Results are based on 50,000 retained posterior draws. Blue shaded area indicates 90 % probability mass. 2 – Computed as square root of inverse-gamma posterior.

Sources: Eurostat, Federal Statistical Office, own calculations

Figure 13 Trend component of hours worked by full-time employees (first row), its volatility (second row), trend growth (third row) and its autoregressive parameters and volatility (fourth row).

Hours worked by part-time workers estimates and projections[1]

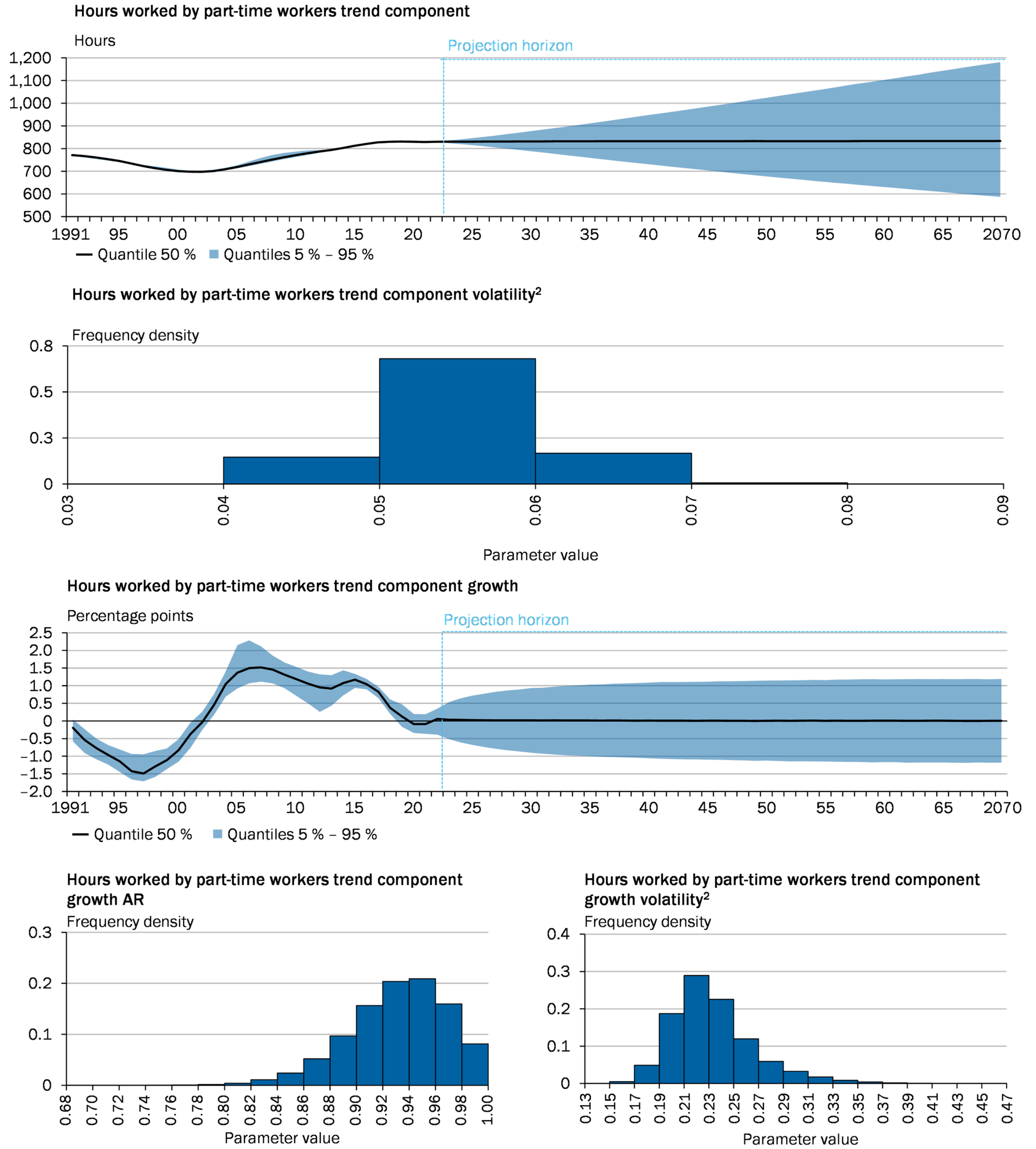

1 – Results are based on 50,000 retained posterior draws. Blue shaded area indicates 90 % probability mass. 2 – Computed as square root of inverse-gamma posterior.

Sources: Eurostat, Federal Statistical Office, own calculations

Figure 14 Trend component of hours worked by part-time employees (first row), its volatility (second row), trend growth (third row) and its autoregressive parameters and volatility (fourth row).

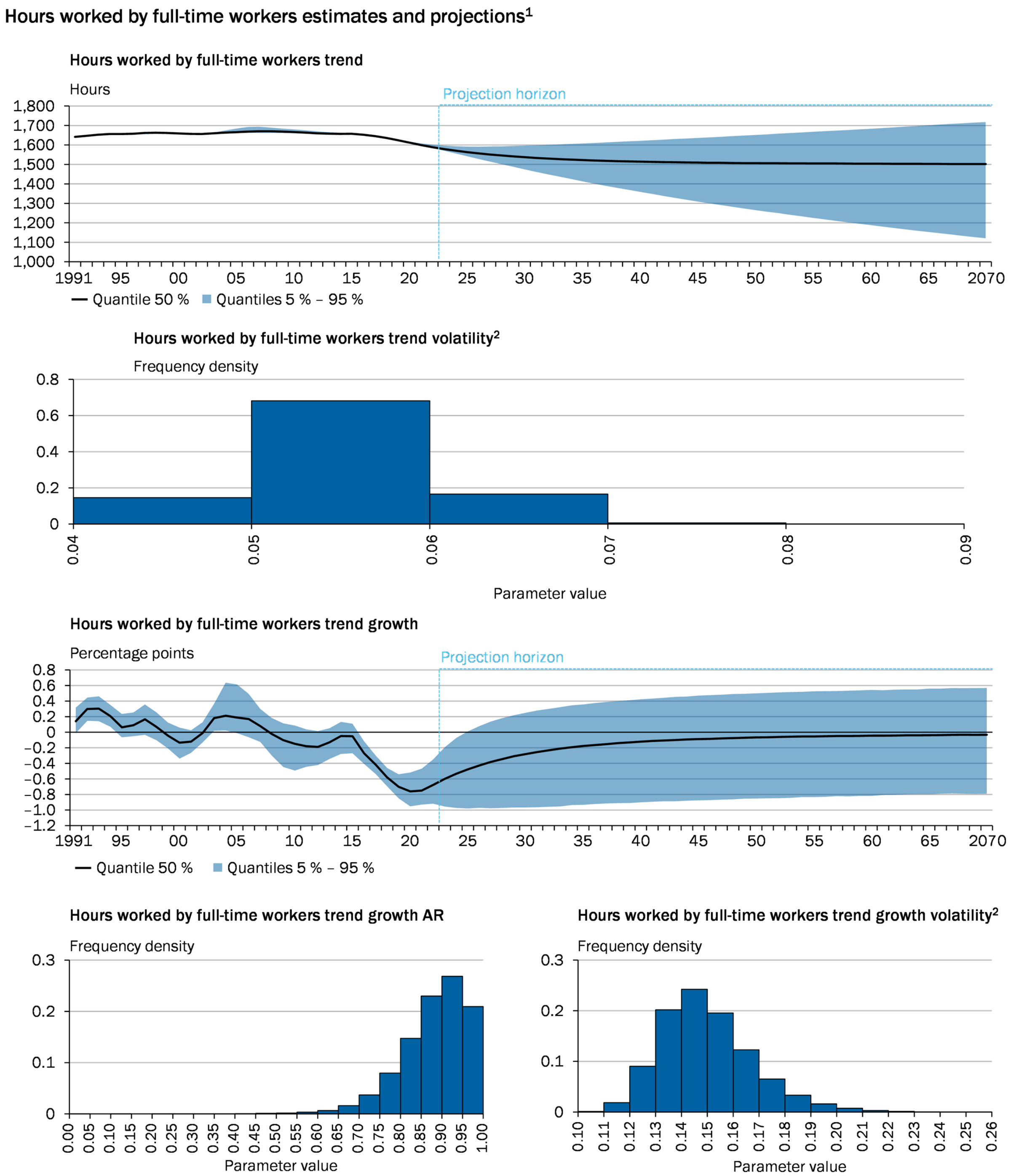

1 – Results are based on 50,000 retained posterior draws. Blue shaded area indicates 90 % probability mass. 2 – Computed as square root of inverse-gamma posterior.

Sources: Eurostat, Federal Statistical Office, own calculations

Figure 15 Trend component of hours worked by self-employed persons (first row), its volatility (second row), trend growth (third row) and its autoregressive parameters and volatility (fourth row).

Self-employment rate estimates and projections[1]

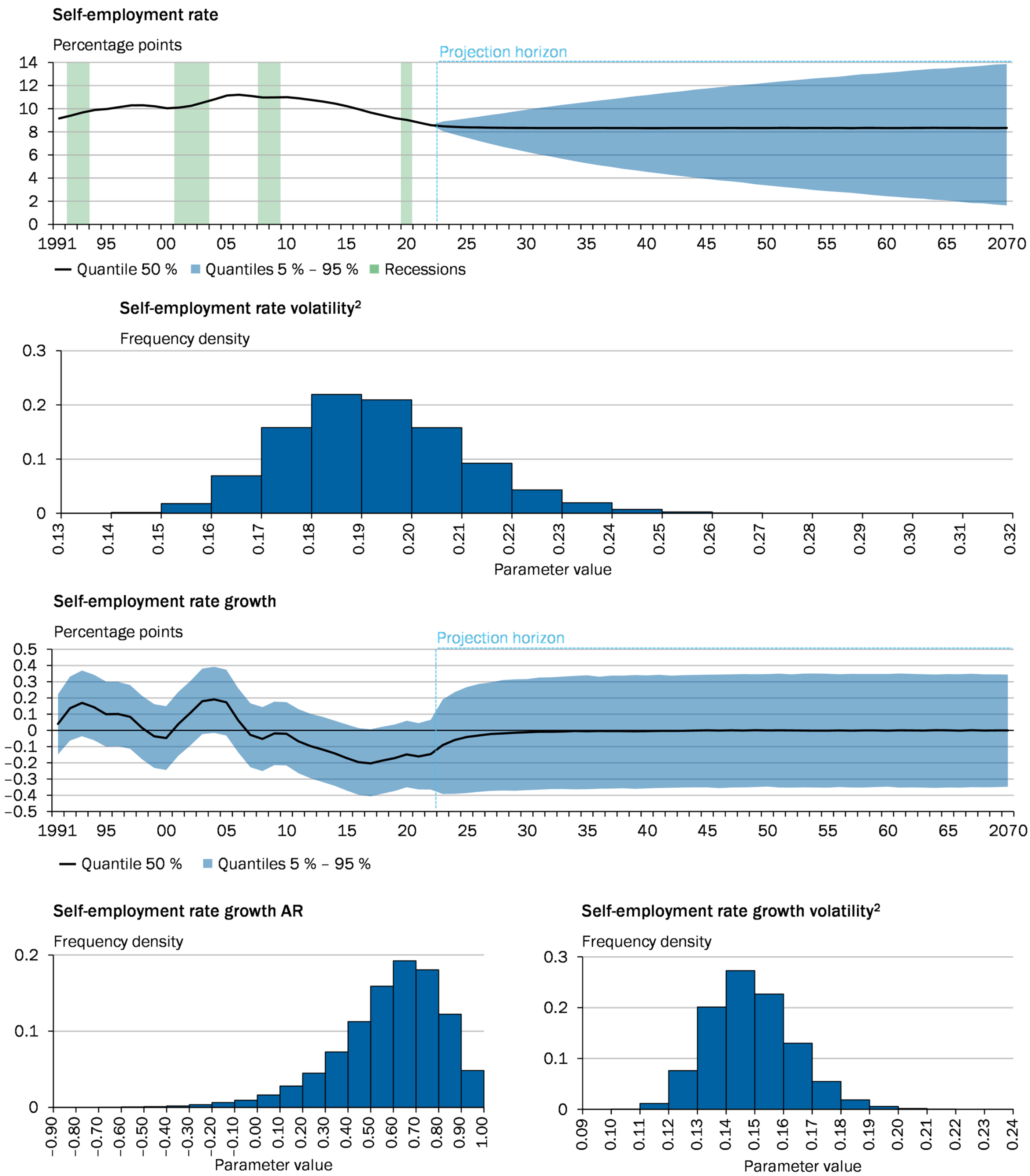

1 – Results are based on 50,000 retained posterior draws. Blue shaded area indicates 90 % probability mass. 2 – Computed as square root of inverse-gamma posterior.

Sources: Eurostat, Federal Statistical Office, own calculations

Figure 16 Self employment rate (first row), its volatility (second row), trend growth (third row) and its autoregressive coefficient and volatility (fourth row).

Part-time rate estimates and projections[1]

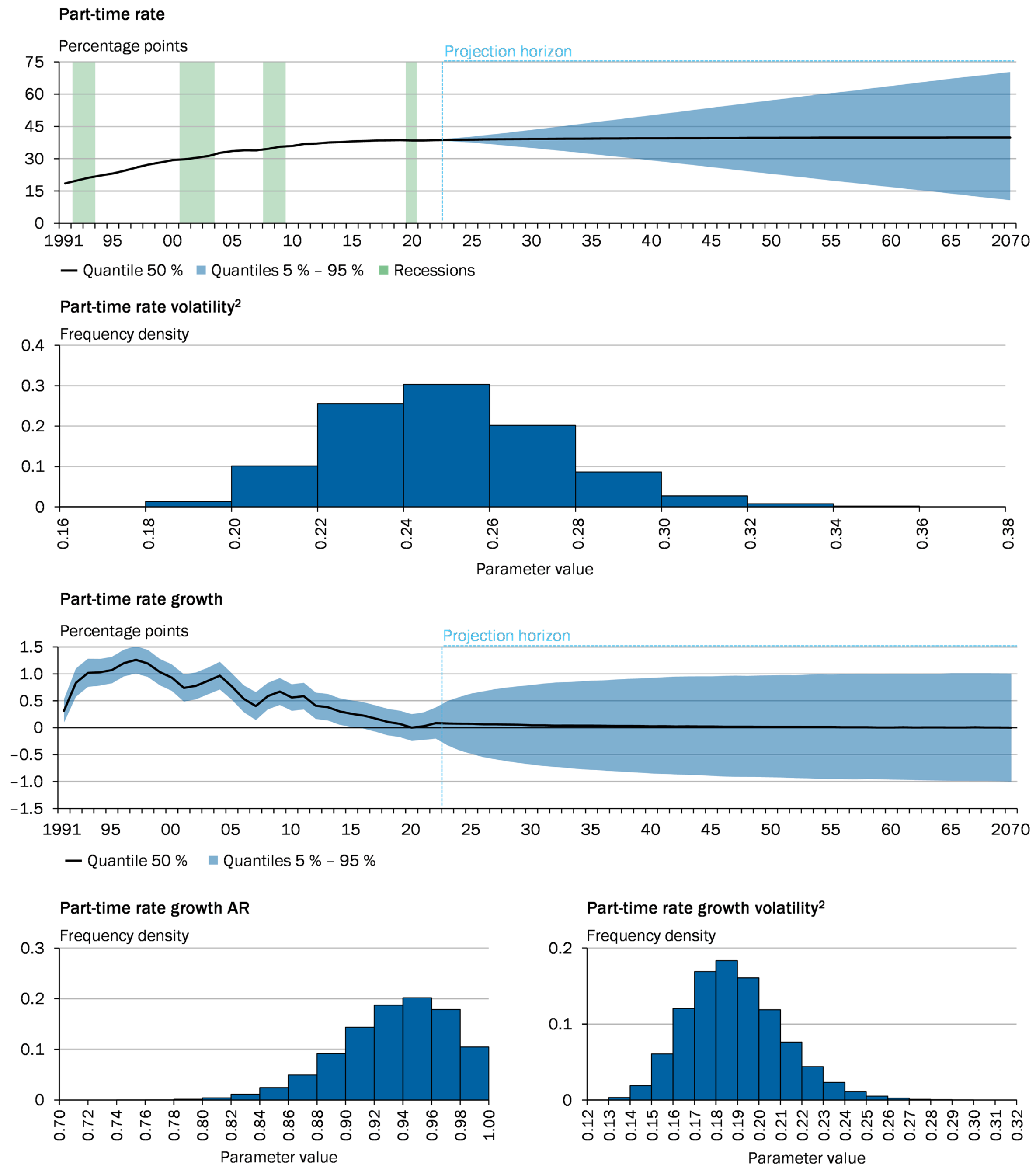

1 – Results are based on 50,000 retained posterior draws. Blue shaded area indicates 90 % probability mass. 2 – Computed as square root of inverse-gamma posterior.

Sources: Eurostat, Federal Statistical Office, own calculations

Figure 17 Part-time employment rate (first row), its volatility (second row), trend growth (third row) and its autoregressive coefficient and volatility (fourth row).

IV.2 Natural Rate of Unemployment

This appendix presents detailed prior specification and estimation results for the non-accelerating inflation rate of unemployment (NAIRU). This component relies on the baseline filter, including a time-varying autoregressive coefficient and an autoregressive trend growth specification. For the sake of interpretation, the time-varying autoregressive coefficient has bounded support over the interval $[0, 1)$. Specification tests show that this coefficient seems to capture most of the non-trend variation, such that including the inflation signal does not improve the fit.

In our analysis, we generate a sample from the condition posterior consisting of 360,000 draws. To ensure the reliability of our findings, we discard the initial 10,000 samples, as they might not accurately reflect the true posterior. To enhance the efficiency of our results and minimize autocorrelation, we select only every seventh sample from the remaining pool. We conducted a comprehensive assessment of the convergence of our sampling method, employing a range of diagnostic tests that included Geweke t-tests and integrated autocorrelation times. The outcomes of these assessments strongly suggest that our sampler has achieved a satisfactory level of convergence. Furthermore, when we examined trace plots, they yielded similar insights into the convergence behavior of our model. Full convergence results are available upon request.

IV.2.1 Prior Distributions

Table 9 summarizes the parameter values for the prior distributions.

					quantiles	
Innovation variances						
			a	b	$\sqrt{\mathcal{Q}(0.01)}$	$\sqrt{\mathcal{Q}(0.99)}$
y_t^τ innovation variance	σ_τ^2	$\mathcal{IG}\,(a.b)$	40	0.3	0.073	0.106
y_t^g innovation variance	σ_g^2	$\mathcal{IG}\,(a.b)$	60	0.05	0.025	0.034
ϕ_t^c innovation variance	$\sigma_{\phi^c}^2$	$\mathcal{IG}\,(a.b)$	10	1	0.231	0.492
ψ_t^c innovation variance	$\sigma_{\psi^c}^2$	$\mathcal{IG}\,(a.b)$	5	4	0.587	1.768
Regression parameters						
					quantiles	
			μ	ξ	$\mathcal{Q}(0.01)$	$\mathcal{Q}(0.99)$
y_t^τ initial state	y_0^τ	calibrated	0.77			
y_t^g initial state	y_0^g	$\mathcal{N}\,(\mu,\xi)$	0	1^2	-2.326	2.326
ϕ_t^c initial state	ϕ_0^c	$\mathcal{TN}\,(\mu,\xi)$	0	10	0.01	0.99
ψ_t^c initial state	ψ_0^c	$\mathcal{N}\,(\mu,\xi)$	0	2^2	-4.653	4.653
Trend bounds						
		parameter value				
y^τ upper trend bound	$\overline{y^\tau}$	100				
y^τ lower trend bound	$\underline{y^\tau}$	0				
ϕ_t^c upper AR bound	$\overline{\phi_t^c}$	1				
ϕ_t^c lower AR bound	$\underline{\phi_t^c}$	0				

Table 9 Prior distributions for relevant innovation variance and regression parameters of the NAIRU model. $\mathcal{Q}(\cdot)$ denotes the quantile function.

IV.2.2 Detailed Estimation and Projection Results

Figures 18 presents detailed estimation and projection results.

German natural rate of unemployment estimates and projections[1]

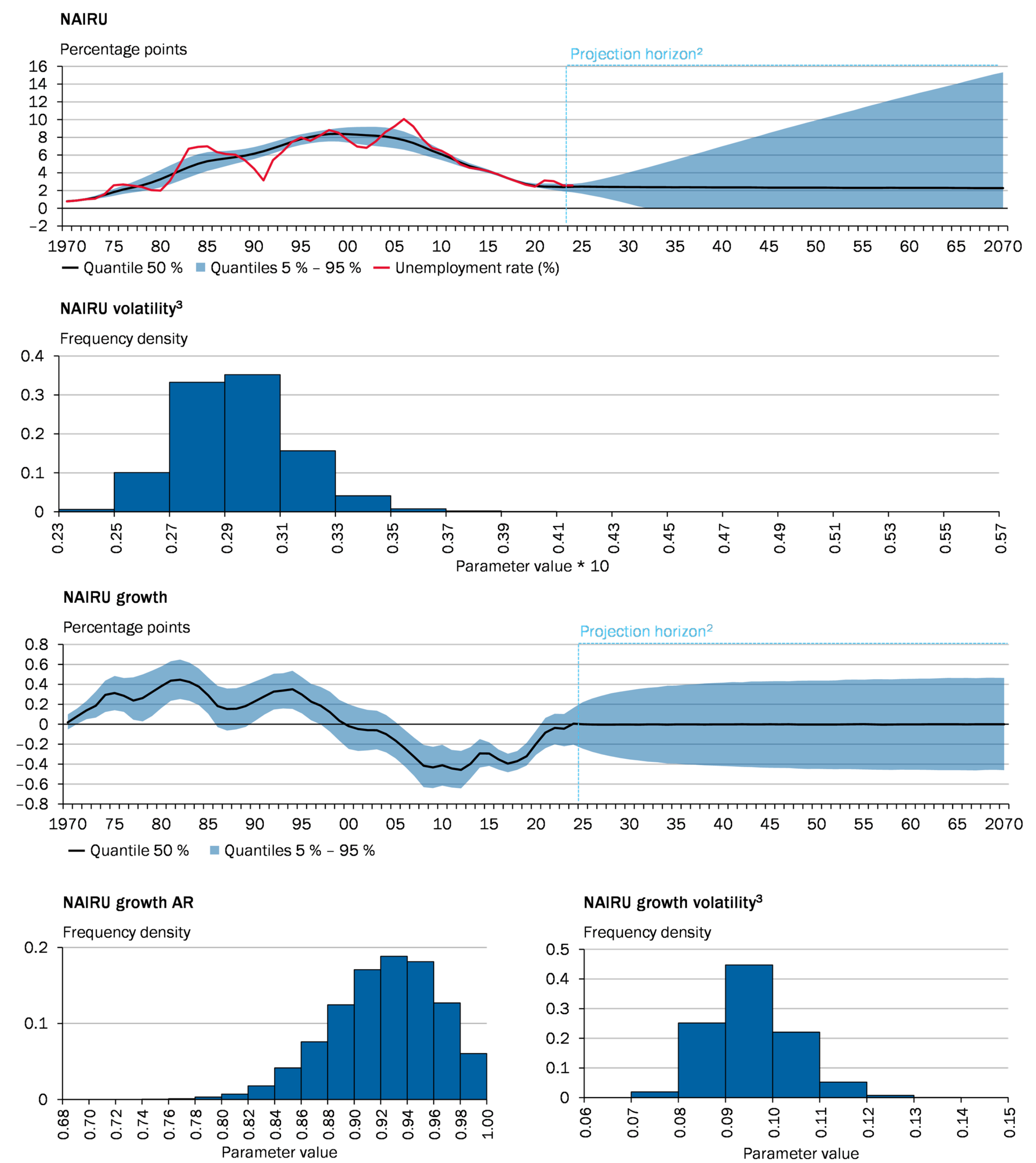

1 – Results are based on 50,000 retained posterior draws. Blue shaded area indicates 90 % probability mass. 2 – Projection horizon is 2025–2070. For 2023 and 2024, we use the GCEE short-run business cycle forecasts and treat them as data. 3 – Computed as square root of inverse-gamma posterior.

Sources: Federal Statistical Office, own calculations

Figure 18 NAIRU and data (first row) and its parameters: volatility (second row), trend growth (third row), its auto-regressive parameter and volatility (fourth row).

IV.3 Labor Participation

This appendix presents detailed prior specification and estimation results for labor participation rates. We assess five age cohorts separately: the yound adults (15-19 year old), the prime work age (20-59 year olds) as well as the early retirement agers (60-64 year olds) and the retirement agers (65-69 as well as 70-74 year olds). In contrast to the baseline filter, we use an AR(1) with intercept specification for trend growth, where the autoregressive coefficient can be easily sampled by means of the Metropolis-Hastings algorithm of Chib and Greenberg (1994) and the intercept can be sampled as a regression parameter in the Gibbs framework. The series are aggregated to workforce level by weighting them with their respective share of the working population.

For our analysis, we generate a total of 360,000 samples from the conditional posterior distributions. In order to ensure the reliability of our results, we exclude the initial 10,000 samples, as they may not accurately represent the true distribution. To improve the efficiency of our dataset and minimize autocorrelation, we select only every seventh sample from the remaining pool. We conducted a rigorous evaluation of the convergence of our sampling method using various diagnostic tests, including Geweke t-tests and integrated autocorrelation times. The outcomes of these tests strongly indicate that our sampler has achieved a satisfactory level of convergence. Furthermore, our examination of trace plots yielded similar insights into the convergence of our model. Full convergence results are available upon request.

IV.3.1 Prior Distributions

Tables 10 and 11 summarizes the parameter values for the prior distributions.

Innovation variances for all models							
						quantiles	
			a	b	$\sqrt{\mathcal{Q}(0.01)}$	$\sqrt{\mathcal{Q}(0.99)}$
participation in age groups 15 - 19 and 60 – 64 years						
y_t^τ innovation variance	σ_τ^2	$\mathcal{IG}\,(a.b)$	50	0.1	0.038	0.053
y_t^g innovation variance	σ_g^2	$\mathcal{IG}\,(a.b)$	30	0.5	0.106	0.163
ψ_t^c innovation variance	$\sigma_{\psi^c}^2$	$\mathcal{IG}\,(a,b)$	5	4	0.587	1.768
remaining models						
y_t^τ innovation variance	σ_τ^2	$\mathcal{IG}\,(a.b)$	50	0.1	0.038	0.053
y_t^g innovation variance	σ_g^2	$\mathcal{IG}\,(a.b)$	40	0.5	0.094	0.137
ψ_t^c innovation variance	$\sigma_{\psi^c}^2$	$\mathcal{IG}\,(a,b)$	5	4	0.587	1.768

Table 10 Prior distributions for relevant innovation variance parameters of labor participation models. $\mathcal{Q}(\cdot)$ denotes the quantile function.

Regression parameters						
					quantiles	
			μ	ξ	$\mathcal{Q}(0.01)$	$\mathcal{Q}(0.99)$
participation in age group 15 - 19 years						
y_t^τ initial state	y_0^τ	calibrated	63.76			
participation in age group 20 - 59 years						
y_t^τ initial state	y_0^τ	calibrated	70.77			
participation in age group 60 - 64 years						
y_t^τ initial state	y_0^τ	calibrated	42.23			
participation in age group 65 - 69 years						
y_t^τ initial state	y_0^τ	calibrated	5.11			
participation in age group 70 - 74 years						
y_t^τ initial state	y_0^τ	calibrated	2.54			
all models						
y_t^g intercept	μ^g	$\mathcal{N}(\mu, \xi)$	0	1^2	-2.326	2.326
y_t^g AR(1)	ϕ^g	$\mathcal{TN}(\mu, \xi)$	0	1^2	-0.972	0.972
ψ_t^c initial state	ψ_0^c	$\mathcal{N}(\mu, \xi)$	0	2^2	-4.653	4.653

Trend bounds for all models		
		parameter value
y^τ upper trend bound	$\overline{y^\tau}$	100
y^τ lower trend bound	$\underline{y^\tau}$	0
ϕ^g upper AR bound	$\overline{\phi^g}$	1
ϕ^g lower AR bound	$\underline{\phi^g}$	-1

Table 11 Prior distributions for relevant regression parameters of labor participation models. $\mathcal{Q}(\cdot)$ denotes the quantile function.

IV.3.2 Detailed Estimation and Projection Results

In the following, we present detailed estimation results.

- Figures 19 presents detailed estimation and projection results for the age cohort of 15-19 year olds.
- Figures 20 presents detailed estimation and projection results for the age cohort of 20-59 year olds.
- Figures 21 presents detailed estimation and projection results for the age cohort of 60-64 year olds.
- Figures 22 presents detailed estimation and projection results for the age cohort of 65-69 year olds.
- Figures 23 presents detailed estimation and projection results for the age cohort of 70-74 year olds.

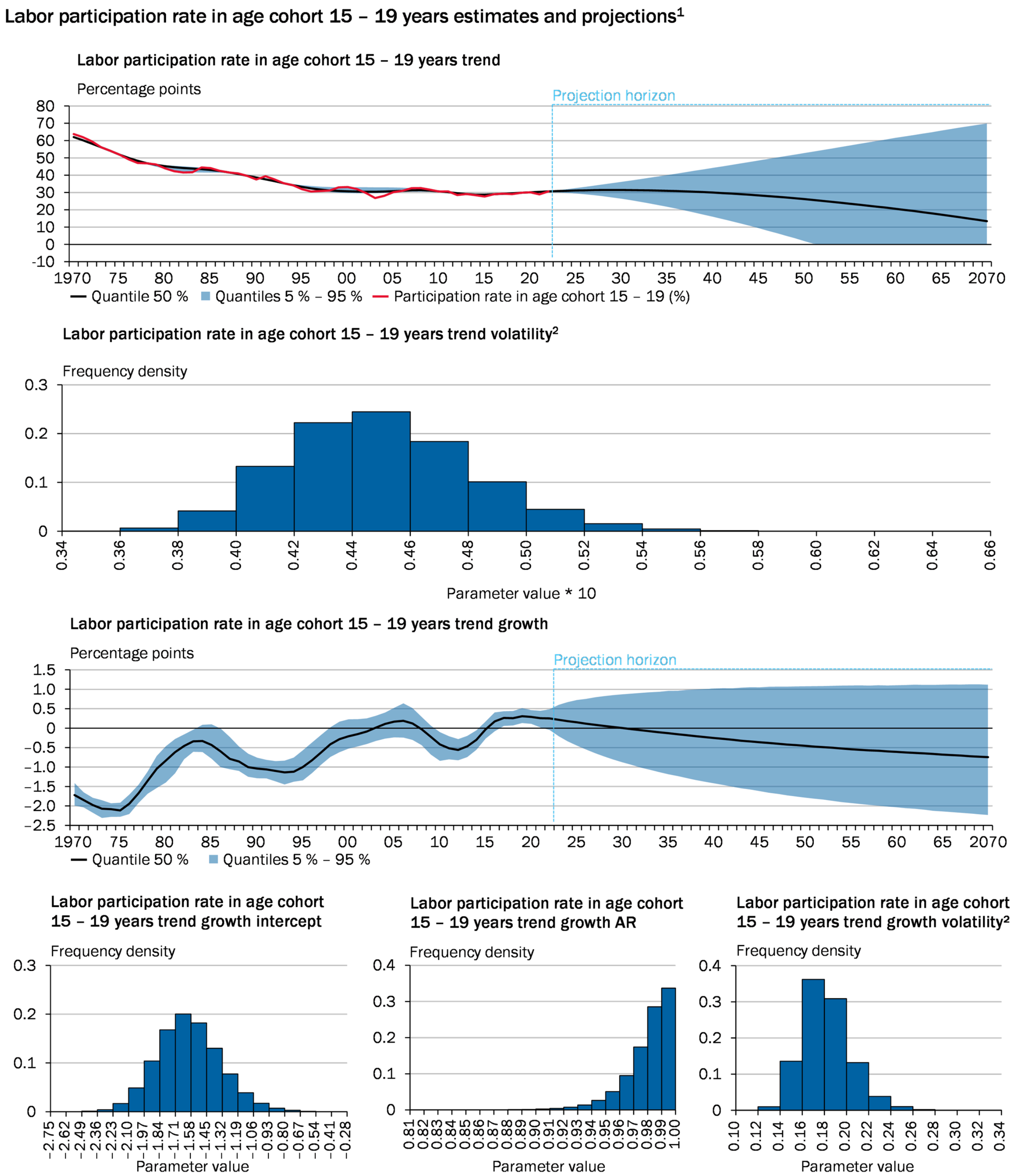

1 – Results are based on 50,000 retained posterior draws. Blue shaded area indicates 90 % probability mass. 2 – Computed as square root of inverse-gamma posterior.

Sources: Eurostat, Federal Statistical Office, OECD, own calculations

Figure 19 Trend of labor participation rate in the age group of 15 - 19 year olds and data (first row) and its parameters: volatility (second row), trend growth (third row), its auto-regressive parameter, intercept and volatility (fourth row).

Labor participation rate in age cohort 20 – 59 years estimates and projections[1]

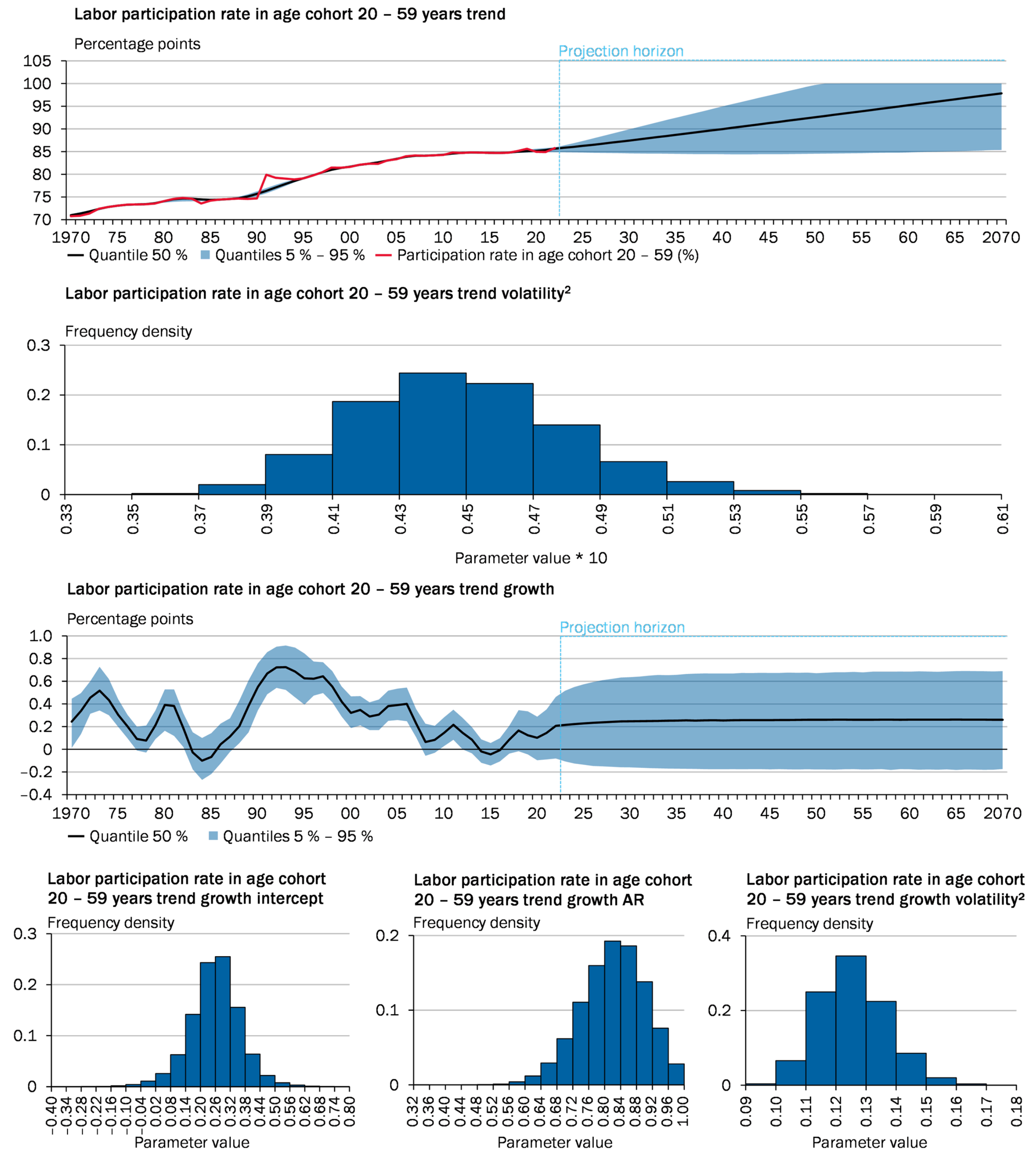

1 – Results are based on 50,000 retained posterior draws. Blue shaded area indicates 90 % probability mass. 2 – Computed as square root of inverse-gamma posterior.

Sources: Eurostat, Federal Statistical Office, OECD, own calculations

Figure 20 Trend of labor participation rate in the age group of 20 - 59 year olds and data (first row) and its parameters: volatility (second row), trend growth (third row), its auto-regressive parameter, intercept and volatility (fourth row).

Labor participation rate in age cohort 60 – 64 years estimates and projections[1]

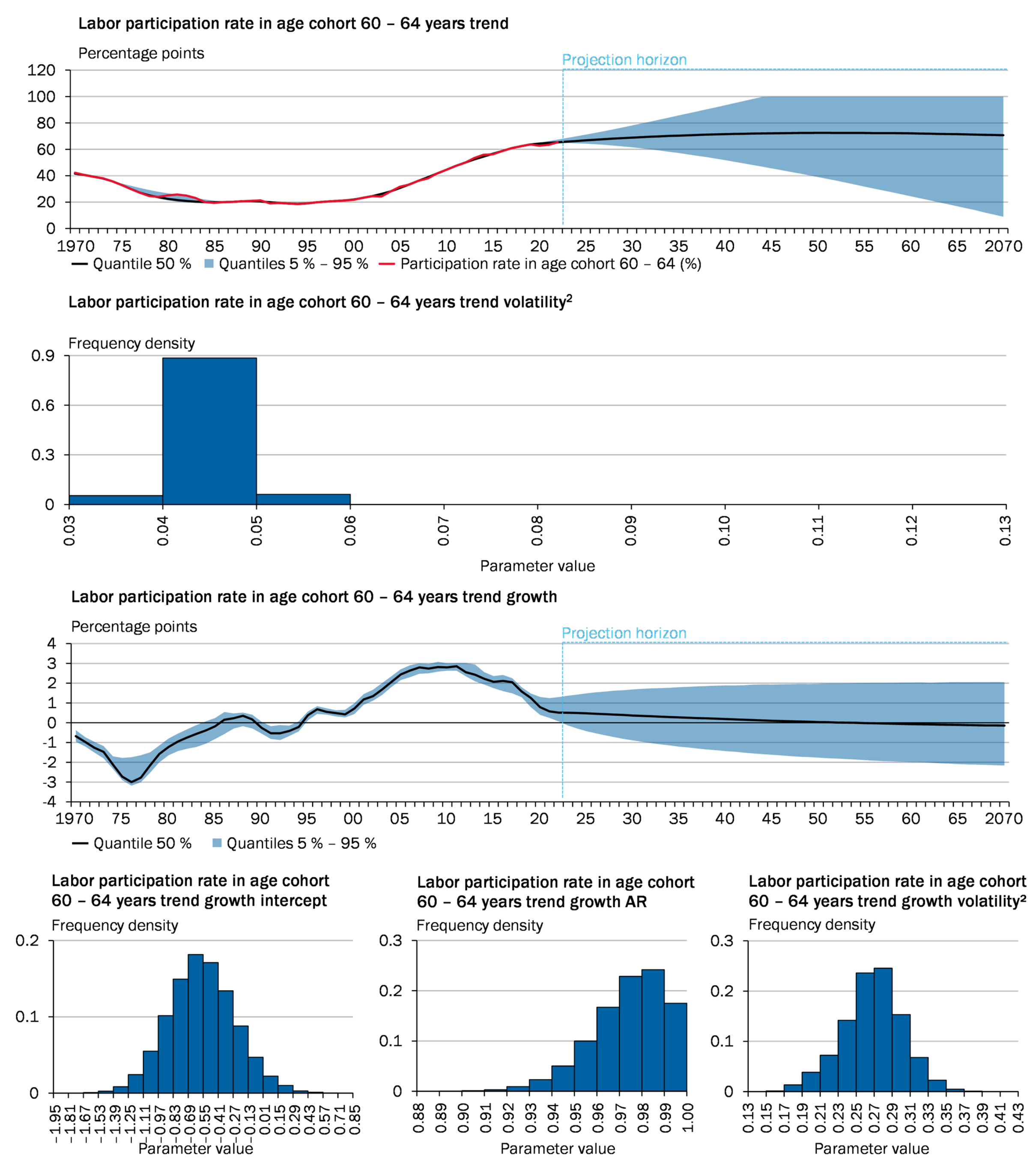

1 – Results are based on 50,000 retained posterior draws. Blue shaded area indicates 90 % probability mass. 2 – Computed as square root of inverse-gamma posterior.

Sources: Eurostat, Federal Statistical Office, OECD, own calculations

Figure 21 Trend of labor participation rate in the age group of 60 - 64 year olds and data (first row) and its parameters: volatility (second row), trend growth (third row), its auto-regressive parameter, intercept and volatility (fourth row).

Labor participation rate in age cohort 65 – 69 years estimates and projections[1]

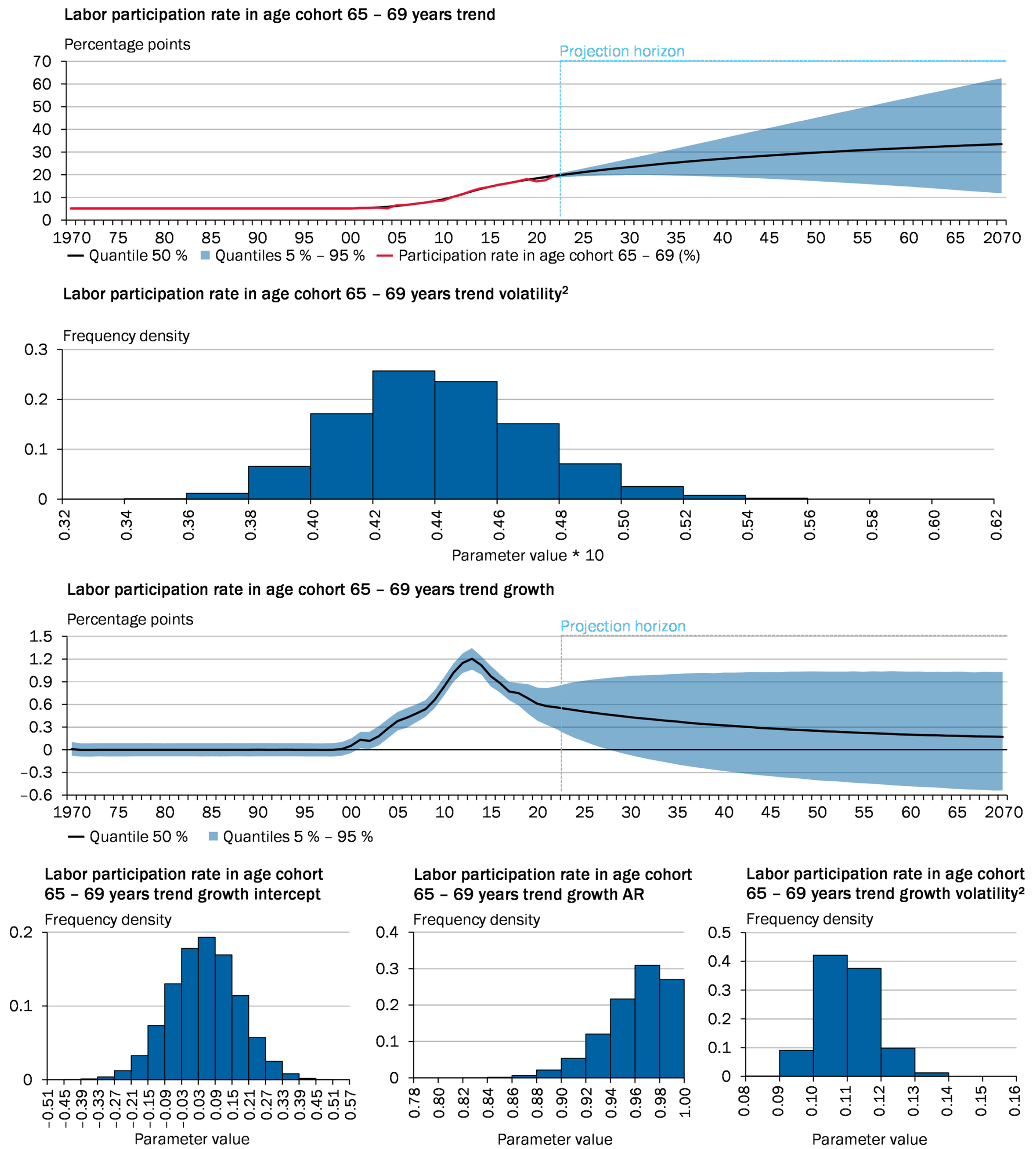

1 – Results are based on 50,000 retained posterior draws. Blue shaded area indicates 90 % probability mass. 2 – Computed as square root of inverse-gamma posterior.

Sources: Eurostat, Federal Statistical Office, OECD, own calculations

Figure 22 Trend of labor participation rate in the age group of 65 - 69 year olds and data (first row) and its parameters: volatility (second row), trend growth (third row), its auto-regressive parameter, intercept and volatility (fourth row).

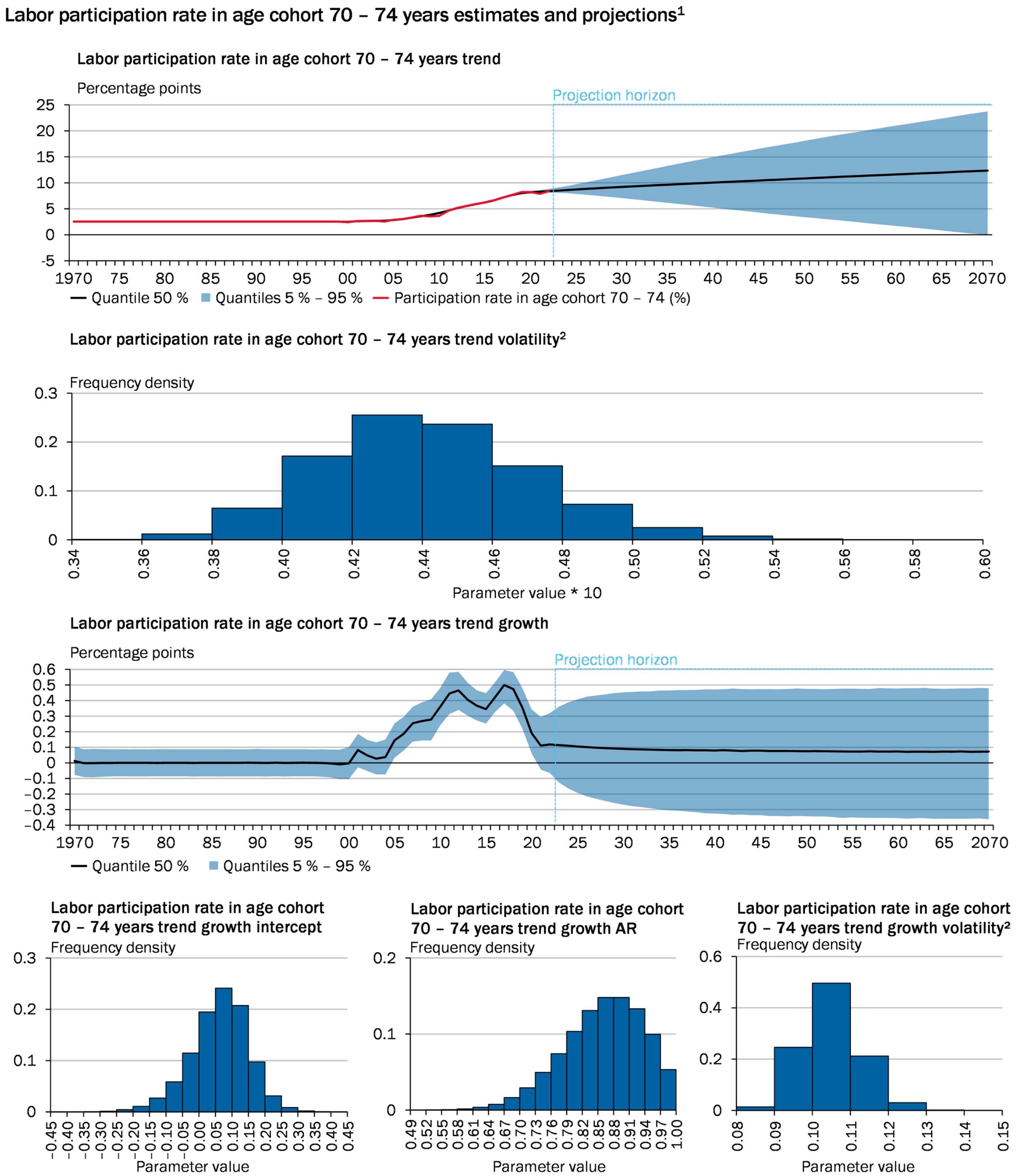

1 – Results are based on 50,000 retained posterior draws. Blue shaded area indicates 90 % probability mass. 2 – Computed as square root of inverse-gamma posterior.

Sources: Eurostat, Federal Statistical Office, OECD, own calculations

Figure 23 Trend of labor participation rate in the age group of 70 - 74 year olds and data (first row) and its parameters: volatility (second row), trend growth (third row), its auto-regressive parameter and volatility (fourth row).

V Human Capital

This appendix presents detailed prior specification and estimation results for human capital. We specify human capital to follow a random walk with a time-varying random-walk drift, as in Appendix **??**. Human capital is approximated by the average years of schooling taken from de la Fuente and Doménech (2006). Before conducting our analysis, we made a transformation to the data. We converted the series into natural logarithms and then scaled the values by multiplying them by 100. We specify human capital as a random walk without a cyclical component. For our analysis, we generate 101,000 samples from the conditional posteriors. To ensure our results are reliable, we discard the initial 1,000 samples as they may not yet represent the true distribution.

V.1 Prior Distributions

Table 12 summarizes information on the prior distributions.

Innovation variances						
					quantiles	
			a	b	$\sqrt{\mathcal{Q}(0.01)}$	$\sqrt{\mathcal{Q}(0.99)}$
y_t^τ innovation variance	σ_τ^2	$\mathcal{IG}\left(a,b\right)$	40	5	0.298	0.432
y_t^g innovation variance	σ_g^2	$\mathcal{IG}\left(a,b\right)$	40	0.1	0.042	0.061
Regression parameters						
					quantiles	
			μ	ξ	$\mathcal{Q}(0.01)$	$\mathcal{Q}(0.99)$
y_t^τ initial state	y_0^τ	calibrated	232.55			
y_t^g initial state	y_0^g	$\mathcal{N}\left(\mu,\xi\right)$	0.91	0.1^2	0.677	1.143
Trend bounds						
		parameter value				
y^τ upper trend bound	$\overline{y^\tau}$	∞				
y^τ lower trend bound	$\underline{y^\tau}$	12				

Table 12 Prior distributions for relevant innovation variance and regression parameters of the human capital model. $\mathcal{Q}(\cdot)$ denotes the quantile function.

V.2 Detailed Estimation and Projection Results

Figure 24 depicts the estimation results.

Human capital estimates and projections[1]

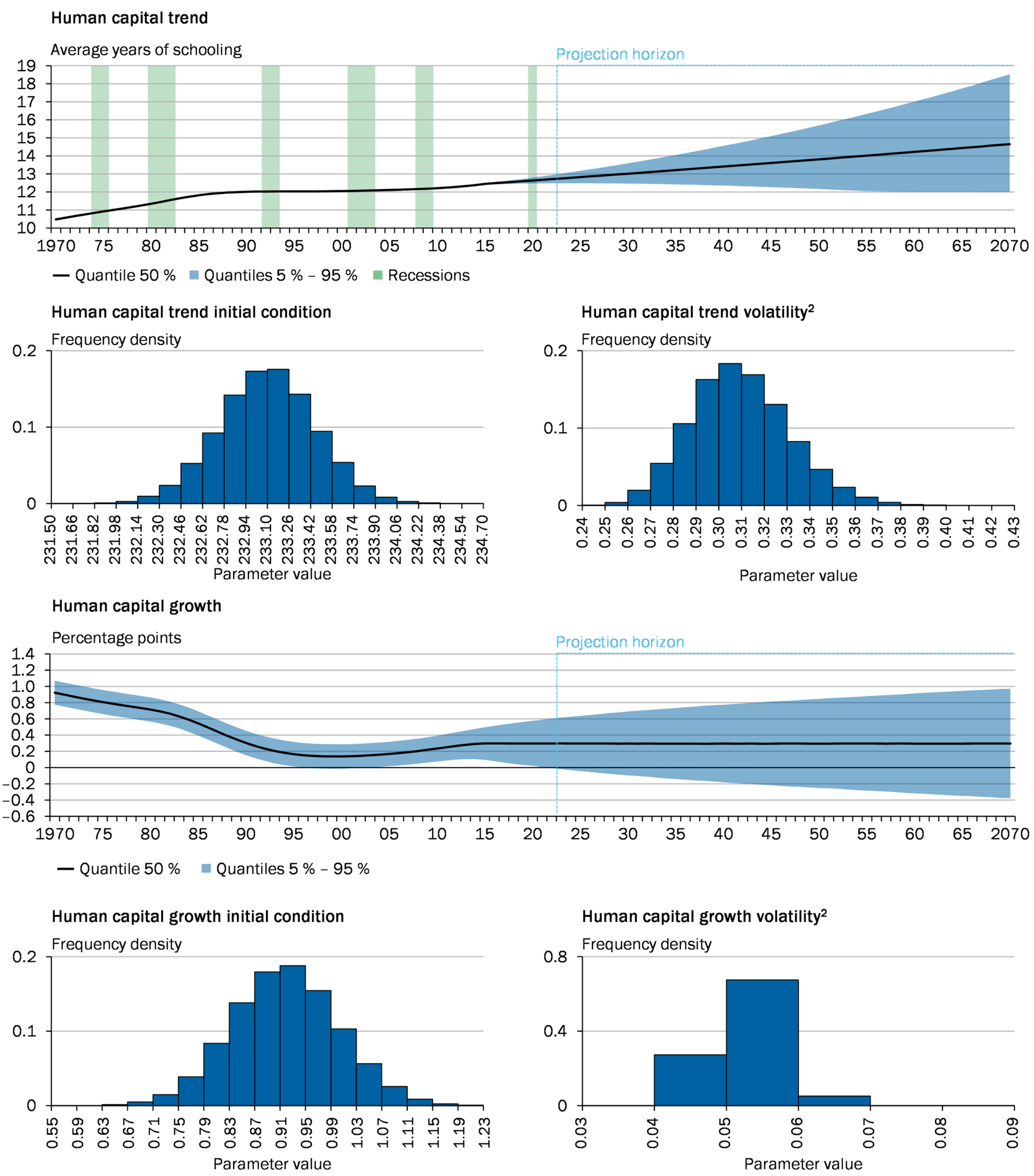

1 – Results are based on 50,000 retained posterior draws. Blue shaded area indicates 90 % probability mass. 2 – Computed as square root of inverse-gamma posterior.

Sources: Federal Statistical Office, own calculations

Figure 24 Human capital (first row), its initial condition and volatility (second row), trend growth (third row) as well as its initial condition and volatility (fourth row).

References

Anger, C., A. Plünnecke, and J. Schmidt (2010): "Bildungsrenditen in Deutschland: Einflussfaktoren, politische Optionen und ökonomische Effekte," *IW-Analysen*, 65.

Berger, T., G. Everaert, and L. Pozzi (2021): "Testing for international business cycles : a multilevel factor model with stochastic factor selection," *Journal of Economic Dynamics Control*, 128.

Breuer, S. and S. Elstner (2020): "Germany's Growth Prospects against the Backdrop of Demographic Change," *Journal of Economics and Statistics*, 240, 565–605.

Chib, S. and E. Greenberg (1994): "Bayes inference in regression models with ARMA (p, q) errors," *Journal of Econometrics*, 64, 183–206.

de la Fuente, A. and R. Doménech (2006): "Human Capital in Growth Regressions: How Much Difference Does Data Quality Make?" *Journal of the European Economic Association*, 4, 1–36.

Havik, K., K. McMorrow, F. Orlandi, C. Planas, R. Raciborski, W. Roeger, A. Rossi, A. Thum-Thysena, and V. Vandermeulen (2014): "The Production Function Methodology for Calculating Potential Growth Rates Output Gaps," *Economic Papers*.

Knetsch, T. A. (2013): "A User Cost Approach to Capital Measurement in Aggregate Production Functions," *Jahrbücher für Nationalökonomie und Statistik*, 233, 638–660.

OECD (2009): *Measuring Capital. OECD Manual*.

Pfeiffer, F. and H. Stichnoth (2021): "Fiscal and individual rates of return to university education with and without graduation," *Applied Economics Letters*, 28, 1432–1435.